

Non-compact Gepner Models, Landau-Ginzburg Orbifolds and Mirror Symmetry

Sujay K. Ashok^{a,b}, Raphael Benichou^c and Jan Troost^c

^aInstitute of Mathematical Sciences
C.I.T Campus, Taramani
Chennai, India 600113

^bPerimeter Institute for Theoretical Physics
Waterloo, Ontario, ON N2L2Y5, Canada

^cLaboratoire de Physique Théorique¹, Ecole Normale Supérieure
24 Rue Lhomond Paris 75005, France

Abstract

We study non-compact Gepner models that preserve sixteen or eight supercharges in type II string theories. In particular, we develop an orbifolded Landau-Ginzburg description of these models analogous to the Landau-Ginzburg formulation of compact Gepner models. The Landau-Ginzburg description provides an easy and direct access to the geometry of the singularity associated to the non-compact Gepner models. Using these tools, we are able to give an intuitive account of the chiral rings of the models, and of the massless moduli in particular. By studying orbifolds of the singular linear dilaton models, we describe mirror pairs of non-compact Gepner models by suitably adapting the Greene-Plesser construction of mirror pairs for the compact case. For particular models, we take a large level, low curvature limit in which we can analyze corrections to a flat space orbifold approximation of the non-compact Gepner models. This gives rise to a counting of moduli which differs from the toric counting in a subtle way.

1 Introduction

Mirror symmetry for Calabi-Yau 3-folds is a subject of great interest to physicists as well as mathematicians [1][2]. Mirror pairs were first exhibited [3] by studying orbifolds of the quintic at the Gepner point [4] in the Calabi-Yau moduli space. This was explored in more detail in [5] which contained the first mathematical predictions from mirror symmetry. Many generalizations were found using the Landau-Ginzburg formulation that were applicable in non-geometric regimes [6].

In this paper, we wish to extend the study of mirror symmetry to non-compact Gepner models. Various approaches towards this problem have been followed. Toric Calabi-Yau manifolds have been very well studied in the literature following the construction of mirror pairs for hypersurfaces in toric varieties [7] and for non-compact Calabi-Yau manifolds (see [8] and references therein). In the physics literature, this has been reformulated using a gauged linear sigma model [9, 10, 11]. Progress has also been made for more general $c = 9$ theories

¹Unité Mixte du CRNS et de l'Ecole Normale Supérieure associée à l'université Pierre et Marie Curie 6, UMR 8549. Preprint LPTENS-07/51.

via conformal field theory techniques [12]. In particular, the work on T-duality for the $N = 2$ cigar and the Liouville conformal field theories is relevant in this context [13, 14, 15, 16].

One of the gaps we aim to fill in this paper is to clarify the link between non-compact Gepner models and their Landau-Ginzburg description. For compact Calabi-Yau manifolds that are hypersurfaces in weighted projective space, the Landau-Ginzburg description is closely tied to the geometry [17]. These are two of the many phases in a gauged linear sigma-model description [9]. The Landau-Ginzburg model is also extremely useful for providing a simple setting to do computations. For instance, it has served well in the past for establishing the link between compact Gepner models and compact Calabi-Yau manifolds [17] as well as to provide the first list of Calabi-Yau hypersurfaces in $WCIP^4$ [18].

Our approach in this paper is to stress the ingredients of the analysis of Gepner models that survive the transition from going from the compact to the non-compact case. We also point out the characteristics that differ in the two cases. Moreover we study in detail the orbifolded Landau-Ginzburg description of these models [19, 20]. This allows us to compare our models with geometric backgrounds which can be used as internal spaces for type II strings on $\mathbb{R}^{3,1}$.

In section 2 we will review the asymptotic partition function of non-compact Gepner models [21, 22, 23, 12, 24]. The asymptotic partition function, which is proportional to the divergent volume of space-time, otherwise behaves much as the partition function in the compact case. In particular we show here that the β -method of Gepner [4] for constructing modular invariants can be adapted to the non-compact case. We then start the discussion of the localized spectrum [22, 12, 24], which is characteristic of non-compact models.

In section 3 we will link the non-compact Gepner models to Landau-Ginzburg models. We briefly remark on the difference between the compact and non-compact Landau-Ginzburg model [25]. For instance, the former gives rise to a unital chiral ring, while the latter gives rise to a ring without unit element. We continue the analysis in section 4 with a discussion of the orbifolds of the Landau-Ginzburg models that are necessary to implement the GSO projection, and other orbifold groups. We will see that the formalism for counting chiral ring elements largely carries over from the compact case [19, 20]. However, it will become intuitive that the Landau-Ginzburg potentials with negative powers exclude some of the (anti-)chiral ring elements as the potential renders them non-normalizable. Continuing the formal counting exercise will turn out to be useful nevertheless. It gives rise to a natural picture of mirror symmetry in conformal field theories, that is strongly reminiscent of its compact counterpart [3, 12]. We will discuss this point in section 6.

In section 5 we provide new examples of mirror conformal field theories. The techniques developed to analyze orbifolded Landau-Ginzburg models come in handy when treating these more complicated models. The mirror pairs of conformal field theories are best understood as linear dilaton backgrounds with $N = 2$ superconformal symmetry. These can be deformed or resolved, to give rise to perturbatively well-defined mirror string backgrounds. Finally, in section 7, we discuss examples in which we can relate the mirror conformal field theories to geometries. It will turn out that we can approximate certain conformal field theories at large level with orbifold singularities that admit a toric description. At infinite level, we find agreement between the conformal field theory and the geometric results. At finite level, we find that the conformal field theory description takes into account various modifications to the background that can lift some moduli. In section 8 we discuss further applications of our results.

2 Non-compact Gepner Models

We start out with a rather brief but technical review of non-compact Gepner models (see e.g. [21, 23, 12, 24]) in order to clarify the fact that the asymptotic partition function of non-compact Gepner models can be constructed using the same tools as in the compact case. We can then lay bare properties of the models along the same lines as in the compact Gepner models. In the second part of this section we give a preview of the ingredients that go into analyzing the localized part of the partition function.

2.1 The Asymptotic Non-compact Gepner Models

For simplicity we will work with type II string theory on $\mathbb{R}^{3,1}$ times an internal (non-compact) conformal field theory of central charge nine². The internal conformal field theory is built from a product of $N = 2$ superconformal field theories. These can be split into three classes depending on whether their central charge is smaller, larger than or equal to three.

- The minimal $N = 2$ superconformal field theories (see e.g. [27]) have central charge smaller than three. They can be viewed as coset conformal field theories of the form $SU(2)_{k-2} \times U(1)_2 / U(1)_k$ of central charge $c_{MM} = 3 - \frac{6}{k}$. The level k is the supersymmetric level of the total $SU(2)$ current algebra present in the parent $N = 1$ Wess-Zumino-Witten model. It is a positive integer larger than or equal to two.

Since the minimal $N = 2$ superconformal models have been reviewed frequently ([28, 29]), and since they are standard in the construction of Gepner models [4], we only very briefly recall some of their properties. The primaries of the model can be labeled by three quantum numbers: the spin j under the $SU(2)_{k-2}$ current algebra, the \mathbb{Z}_{2k} valued chiral momentum n under the $U(1)_k$ current algebra and the \mathbb{Z}_4 valued chiral momentum s labeling a representation of the $U(1)_2$ current algebra. They satisfy the selection rule: $2j \equiv n + s$ [2]. We moreover have an equivalence between the following representations: $(j, n, s) \equiv (\frac{k-2}{2} - j, n - k, s + 2)$. The left-moving $U(1)_R$ charge Q_{MM} for a primary is equal to $Q_{MM} = \frac{n}{k} + \frac{s}{2}$.

- The second class of theories has central charge larger than three. An example in this class is an $N = 2$ linear dilaton theory with a slope such that the central charge is equal to $c = 3 + \frac{6}{l}$ with positive and real values for the parameter l . The superconformal algebra with central charge larger than three has continuous unitary representations which are conveniently labeled [30] by a Casimir $j = 1/2 + ip$ where $p \in \mathbb{R}^+$, by an integer momentum $2m \in \mathbb{Z}$ and a \mathbb{Z}_4 fermionic quantum number s . The left-moving R-charge Q_{nc} of a primary is $Q_{nc} = \frac{2m}{l} + \frac{s}{2}$. (See e.g. [16] for a detailed discussion.)
- The $N = 2$ superconformal algebra with $c = 3$ is exceptional, and can be represented for instance by free scalars (which can realize compact or non-compact target space directions).

In order to mimic the Gepner construction, we will assume that in the case $c > 3$, the chiral algebra has some more structure (see e.g. [21]). For simplicity we will work under the assumption that the parameter l is a positive integer³. We can then add to the chiral

²The constructions can be extended to lower-dimensional flat spaces and to heterotic string theories, with little effort and lots of indices.

³It is sufficient to suppose that the central charge is parameterized by a positive fractional level l [21].

algebra the generator of spectral flow on the $N = 2$ superconformal algebra by $2l$ units. The characters of the extended $N = 2$ superconformal algebra in the continuous representations are given by:

$$Ch_{cont}(j, 2m, s) = q^{\frac{p^2}{l}} \frac{1}{\eta^3(\tau)} \Theta_{s,2}(\tau) \Theta_{2m,l}(\tau). \quad (2.1)$$

It is crucial to us that the modular transformation properties of the characters hinge upon the presence of the θ -functions at levels 2 and l .

2.1.1 Levels And Charge Lattice

We observe that the characters of the $N = 2$ minimal models at level k transform as θ -functions at levels 2 and $-k$, while the extended characters of the $N = 2$ models with central charge $c = 3 + \frac{6}{l}$ transform as θ -functions at level 2 and $+l$. We thus note a first important sign difference in the transformation rules of the characters. Modular invariants in the continuous sector of the theory can be based on modular invariants of θ -functions. For one $U(1)_k$ current algebra at level k these are well-known to correspond to the divisors of k via orbifolding of the diagonal modular invariant. For a product of θ -functions, the analysis is more complicated, but a large class of modular invariants can be constructed by taking products of modular invariants of the factors, and then orbifolding.

In order to write down the modular invariant partition functions, it is useful to introduce a charge lattice for the various $U(1)$ current algebras in the theory. We introduce a vector of levels $(2, 2, \dots, 2; k_1, \dots, k_p; l_1, \dots, l_q)$ where p is the number of minimal model factors, q is the number of non-compact factors, while the number of fermionic levels equal to 2 is $1 + q + p$. Indeed, we work in light-cone gauge on $\mathbb{R}^{3,1}$ such that there is one complex fermion associated to the flat space directions (and there is one complex fermion per factor model). The charge lattice is periodic. In each direction, the periodicity is twice the level. A point in the lattice is defined by a charge vector $r = (s_0, s_1, \dots, s_{p+q}; n_1, \dots, n_p; 2m_1, \dots, 2m_q)$ where we used the notation s_0 for the charge of the flat space fermions under the $U(1)_2$ current algebra, and similarly for the other fermions, while we copy the traditional notation for the chiral momentum quantum numbers of compact and non-compact factors that we introduced above (including their normalization). The scalar product on the charge lattice is defined as follows:

$$\begin{aligned} r^{(1)} \cdot r^{(2)} = & -\frac{s_0^{(1)} s_0^{(2)}}{4} - \frac{s_1^{(1)} s_1^{(2)}}{4} - \dots - \frac{s_{p+q}^{(1)} s_{p+q}^{(2)}}{4} \\ & + \frac{n_1^{(1)} n_1^{(2)}}{2k_1} + \dots + \frac{n_p^{(1)} n_p^{(2)}}{2k_p} \\ & - \frac{(2m_1^{(1)})(2m_1^{(2)})}{2l_1} - \dots - \frac{(2m_q^{(1)})(2m_q^{(2)})}{2l_q}. \end{aligned} \quad (2.2)$$

The contribution of the chiral momenta corresponding to the non-compact factors comes with an opposite sign from those of the compact factors. The all-important signature of the quadratic form is therefore $(-, \dots, -; +, \dots, +; -, \dots, -)$.

2.1.2 A Canonical Vector

We introduce the following vector β_0 in the charge lattice⁴:

$$\beta_0 = (-1, -1, \dots, -1; 1, 1, \dots, 1; -1, -1, \dots, -1). \quad (2.3)$$

We have that the left-moving R-charge Q for a primary state with charge vector r is equal to $Q = 2\beta_0 \cdot r$. We moreover have that

$$\begin{aligned} \beta_0 \cdot \beta_0 &= -\frac{1+p+q}{4} + \sum_{i=1}^p \frac{1}{2k_i} - \sum_{j=1}^q \frac{1}{2l_j} \\ &= -1 \end{aligned} \quad (2.4)$$

where we used that the total central charge of the light-cone gauge conformal field theory is equal to

$$12 = 3(1+p+q) - \sum_{i=1}^p \frac{6}{k_i} + \sum_{j=1}^q \frac{6}{l_j}. \quad (2.5)$$

In summary, the vector β_0 is useful to measure the R-charge, and squares to minus one.

For the right-movers we will always take identical conventions to the left-movers. In particular, the $N = 2$ superconformal algebras have the same structure constants. We will also define the right-moving R-charge of the minimal model factors to be $\tilde{Q}_{MM} = \frac{\tilde{n}}{k} + \frac{\tilde{s}}{2}$ and for the non-compact factors $\tilde{Q}_{nc} = \frac{2\tilde{m}}{k} + \frac{\tilde{s}}{2}$, while the charge vector for the right-movers is $\tilde{r} = (\tilde{s}_0, \dots, ; \dots; \dots, 2\tilde{m}_{p+q})$. So, for the right-movers as well we have that the total $U(1)_R$ charge is given by $\tilde{Q} = 2\beta_0 \cdot \tilde{r}$ with the same vector β_0 .

2.1.3 Products of θ -functions

We define the following notation for the product of characters of the flat space fermions, the minimal model and the non-minimal $N = 2$ superconformal field theories. Since the characters transform like θ -functions, we introduce the symbol:

$$\Theta_r(\tau) = \Theta_{s_0, 2}(\tau) \prod_{i=1}^p \chi_{j_i, n_i, s_i}(\tau) \prod_{i=1}^q Ch_{cont}(j_{p+i}, 2m_i, s_{p+i})(\tau) \quad (2.6)$$

where r is the total charge vector, and the first factor corresponds to the flat space fermions, while the following p factors correspond to minimal model characters, and the final q factors to the non-compact continuous extended characters. In the Θ symbol we have left implicit the labels corresponding to the levels, as well as those corresponding to the Casimirs of the minimal and non-minimal models. The important point is that the Θ -functions transform as a product of ordinary θ -functions under modular transformations.

We introduce now the first modular invariant partition function which is the diagonal modular invariant:

$$Z_{diag} = \sum_r \Theta_r(\tau) \Theta_r(\bar{\tau}), \quad (2.7)$$

⁴We take the entries for the fermions to be minus one, in order to accord with the convention that the left-moving $U(1)_R$ charge is given for instance for a minimal model factor by $Q_{MM} = \frac{n}{k} + \frac{s}{2}$.

where the diagonal sum over r is over all inequivalent charges in the charge lattice. Implicitly, we take a diagonal A-type modular invariant for the Casimir invariants j for all factors⁵. We have suppressed the divergent non-compact volume factor in the formula for the asymptotic partition function.

2.1.4 Locality Orbifold

Now that we have set-up our theory in a way which is very analogous to [4], we can follow that reference closely. Along the way, we reformulate a few minor points in a more modern orbifold language.

Locality in string theory only allows for fermions having either Neveu-Schwarz (NS) or Ramond (R) boundary conditions for all factors simultaneously for the left- or the right-movers. We implement that locality constraint by orbifolding the diagonal partition function by a diagonal $(\mathbb{Z}_2)^{p+q}$ group. The i 'th \mathbb{Z}_2 acts on a state with charge vectors r and \tilde{r} as $(-1)^{(s_0+s_i+\tilde{s}_0+\tilde{s}_i)/2}$ for $i = 1, \dots, p+q$. The action can be summarized by introducing vectors β_i which have a 2 as the first and the $i+1$ 'th entry for $i = 1, \dots, p+q$. Then the action can equivalently be written as $(-1)^{\beta_i \cdot (r+\tilde{r})}$. On an untwisted state with charges s_0 and s_i , the action is the multiplication by a phase $(-1)^{s_0+s_i}$.

The states invariant under $(\mathbb{Z}_2)^{p+q}$ will be purely NS or purely R for the left-movers. Since the partition function was diagonal, the same condition will hold for the right-movers. The orbifold also introduces twisted states. These have left- and right-moving charge vectors that differ by multiples of the vectors β_i [4]. Indeed, since the fermion number s_i is defined modulo four, this introduces a twisted state sector for each \mathbb{Z}_2 orbifold factor, and moreover, since $\beta_i^2 = 2$, we have that the twisted states we introduce in this fashion are also orbifold invariant [4]. Each of the \mathbb{Z}_2 orbifolds introduces twisted states, which renders the sum over left- and right-moving fermion numbers s_i and \tilde{s}_i independent, except for the fact that they need to be of the same parity as the flat space fermion numbers s_0 and \tilde{s}_0 respectively. The above prescription is equivalent to the standard orbifold procedure and produces a new modular invariant partition function. Note that the flat space fermion quantum numbers s_0 and \tilde{s}_0 are still of equal parity. We therefore only have NSNS and RR states at this point. The sum over the left- and right-moving worldsheet fermion numbers s_0 and \tilde{s}_0 will become decoupled after performing a final \mathbb{Z}_2 GSO projection, thus introducing fermions.

2.1.5 Integer R-charge Orbifold

The standard GSO projection in string theory is based on the fact that the partition function only has integer R-charges. In order to ensure this condition in a Gepner model, we perform yet another orbifold. The orbifold action on a state with charge r and \tilde{r} will be $\exp(2\pi i \beta_0 \cdot (r + \tilde{r}))$. We first note that $\beta_0 \cdot \beta_i$ is an integer, such that the action of the orbifold on β_i twisted sectors is identical to the action on β_i untwisted sectors. The order of the $2\beta_0$ orbifold is therefore the order of the operator $e^{2\pi i Q}$ in the untwisted theory (where Q is the total left-moving R-charge in light-cone gauge)⁶. The order of that orbifold is the smallest common divisor d of all the levels in the theory (including the fermionic level 2 when $p+q$ is even and not when $p+q$ is odd).

⁵It would be interesting to study the more general modular invariants of type D and/or type E for the compact factors.

⁶The theory we start out with obeys the charge relation $r = \tilde{r}$. Since $\beta_0 \cdot \beta_i \in \mathbb{Z}$, we still have the relation $e^{2\pi i(Q+\tilde{Q})/2} = e^{2\pi i Q}$ after the (\mathbb{Z}_2^{p+q}) orbifold.

It is clear in the untwisted sector that the orbifold forces the left-moving (and right-moving) $U(1)_R$ charge to be integer. There are also $d - 1$ twisted sectors which have charge vectors which differ by multiples of $2\beta_0$. Since $\beta_0^2 = -1$, we have that these twisted sectors also have integer left- and right-moving R-charges. Thus, the orbifold has provided us with a new modular invariant partition function with integer R-charges for both left- and right-movers. If we introduce the lattice Λ generated by the vectors β_i and $2\beta_0$, then we can write the partition function of the theory as⁷:

$$Z_0 = \sum_{r-\tilde{r} \in \Lambda} \Theta_r(\tau) \Theta_{\tilde{r}}(\bar{\tau}), \quad (2.8)$$

where we restrict the sum to invariant states, namely states obeying the conditions $r \cdot \beta_i \in \mathbb{Z}$ (purely NS or purely R) and $r \cdot 2\beta_0 \in \mathbb{Z}$ (integer R-charges). Again we have left implicit the diagonal A-type invariant for the minimal models as well as the diagonal integral over radial momenta for the compact factors that diverges like the volume of space-time.

2.1.6 The Standard GSO Projection

The partition function now has integer R-charges for all states, and can be GSO projected in the same manner as the flat space partition function. We project onto odd R-charges, i.e. we satisfy the condition $2\beta_0 \cdot r \in 2\mathbb{Z} + 1$ as well as $2\beta_0 \cdot \tilde{r} \in 2\mathbb{Z} + 1$. The charge difference between left- and right-movers for the twisted states is proportional to an odd multiple of β_0 . The twisted sectors are the NS-R and R-NS sectors of the theory, which correspond to space-time fermions, and contribute negatively to the space-time partition function thus implementing space-time statistics. For type II theories, we have obtained an asymptotic supersymmetric partition function in the Gepner formalism. Strictly speaking we have a type IIB partition function, since we have made no distinction between left- and right-movers. It can be transformed easily into a type IIA partition function by flipping the chirality of the final GSO projection for the right-movers in the R-sector.

2.1.7 Discrete Symmetries

In this subsection, we can follow [3] closely since we have set up our model as in the compact case. It is interesting to single out a particular symmetry group of the model.

The symmetry of the compact models contains a $\mathbb{Z}_{k_i} \times \mathbb{Z}_{k_i}$ group. Only the diagonal \mathbb{Z}_{k_i} subgroup has a non-trivial action on a model with diagonal spectrum. This subgroup acts as

$$\Phi_{r,\tilde{r}} \rightarrow \exp(2\pi i(n_i + \tilde{n}_i)/2k_i) \Phi_{r,\tilde{r}}. \quad (2.9)$$

We can introduce a vector

$$\gamma_i = (0, \dots, 0; 0, \dots, 0, 2, 0, \dots, 0; 0, \dots, 0) \quad (2.10)$$

where 2 is in the i 'th entry after the first semi-column. The vector codes the action of the symmetry group as follows:

$$\Phi_{r,\tilde{r}} \rightarrow \exp(\pi i \gamma_i \cdot (r + \tilde{r})) \Phi_{r,\tilde{r}}. \quad (2.11)$$

⁷This partition function for non-compact models is the analogue of Z_0 in [3] for compact Gepner models.

We have a similar action in the non-compact theories. There is a symmetry group $\mathbb{Z}_{l_i} \times \mathbb{Z}_{l_i}$, of which only the diagonal subgroup acts nontrivially on the states. In the full Gepner model, we can think of the product of the diagonal subgroups

$$D = \prod_{i=1}^p \mathbb{Z}_{k_i} \times \prod_{j=1}^q \mathbb{Z}_{l_j} \quad (2.12)$$

as mapped into the charge lattice via the maps $\gamma_{i=1, \dots, p+q}$.

Now we define the operator g_0 that acts by multiplication by $\exp(2\pi i \beta_0 \cdot (r + \tilde{r}))$. It generates a group \mathbb{Z}_d , that we used previously to perform the integer R-charge orbifold. This orbifold group \mathbb{Z}_d contains a subgroup generated by g_0^2 , which is a subgroup of D . Indeed, the element g_0^2 corresponds to a β -vector that has zero fermionic entries. When the order d of the group \mathbb{Z}_d is even, the subgroup generated by g_0^2 has order $n = d/2$ and it has order $n = d$ when d is odd (see also [3]). The part of the diagonal symmetry group D that still acts after the projection onto integer R-charges is

$$G = \left(\prod_{i=1}^p \mathbb{Z}_{k_i} \times \prod_{j=1}^q \mathbb{Z}_{l_j} \right) / \mathbb{Z}_n. \quad (2.13)$$

Following [3] we then define the maximal subgroup H of G which preserves supersymmetry in space-time. This is the subgroup corresponding to all vectors β_m in the charge lattice that satisfy the equation $2\beta_m \cdot \beta_0 \in 2\mathbb{Z}$. This condition ensures that the left- and right- moving R-charges only differ by even integers, as required by supersymmetry. If we write

$$\beta_m = \sum_i c_m^i \gamma_i, \quad (2.14)$$

then this condition boils down to the condition that [3]

$$\sum \frac{c_m^i}{k_i} + \sum \frac{c_m^j}{l_j} \in \mathbb{Z}. \quad (2.15)$$

The subgroup H generated by the vectors β_m that satisfy this condition is the maximal orbifold group consistent with space-time supersymmetry.

Any subgroup F of H can be used to generate new supersymmetric orbifold models. Precisely as in the compact case, modding out the original model by the maximal subgroup H generates the mirror model (in the conformal field theory sense). Moreover, orbifolding by a subgroup F will generate a model that is mirror to the orbifold of the original model by H/F . This was argued in [3] for the compact case, and we will show in section 6 that it is also true for the non-compact models. Note that the mirror symmetry in the conformal field theory that we have set up above holds for *undeformed* models. We will see that deformations of a model are mapped to resolutions of the mirror. We will discuss this important point in greater detail later on.

2.2 The Deep-throat Region Of Non-compact Gepner Models

Until now we have discussed only the continuous part of the spectrum of the non-compact Gepner models. The contribution of these states to the partition function is proportional to the volume of the target space.

A good starting point for the rest of our discussion will be to think of the initial model as based on a product of $N = 2$ superconformal minimal models and $N = 2$ linear dilaton theories.

It is important to observe that although the exact torus partition function exists for these conformal field theories, they only describe the asymptotic spectrum of the corresponding string theory. Indeed, there is a region in space-time that is strongly coupled (due to the linearly growing dilaton in one or several directions). In that region, the one-loop spectrum is not a meaningful quantity.

Nevertheless, we can get a handle on possible deformations of that singular string theory by working under the following hypotheses. We look for local deformations in the strongly coupled region deep in the throat(s). Secondly, we focus on marginal deformations of the worldsheet theory that preserve supersymmetry in space-time. The $N = 2$ superconformal algebra on the worldsheet will be preserved, and the deformations will be based on chiral (or anti-chiral) primaries. Moreover, we suppose that the deformations cannot have $U(1)_R$ quantum numbers that differ from those already appearing in the asymptotic partition function, namely, the charges are quantized as in the asymptotic partition function. We believe all of these are mild assumptions, given space-time supersymmetry. (See e.g. [31] [32] for similar reasonings, mostly from a space-time perspective.)

Using the fact that there is a map between $N = 2$ superconformal algebra representations and representations of $SL(2, \mathbb{R})$ [30], we can reformulate the above conditions as saying that the marginal operators in the full theory should be based on chiral primaries of dimension smaller or equal to one half in the linear dilaton factors. The operator in the linear dilaton factor should have a conformal dimension equal to $h = |m|/k$ where the $U(1)_R$ charge is given by $Q = 2m/k$, and where $2m$ is an allowed $U(1)_R$ quantum number given the (fixed) asymptotic partition function. We get an upper cut-off: $2|m| \leq k$ from the requirement of relevance on the worldsheet. Moreover, we want to study operators that are normalizable at weak coupling. Strict normalisability requires $2|m| > 1$. In particular the value $2m = 0$ is excluded in the non-compact factors, since this would correspond to a non-normalizable operator for a conformal field theory with a non-compact target space. In summary, the quantum number $2|m|$ has to lie in the range $1 < 2|m| \leq k$. It should be noted that the operator with $2|m| = 1$ is on the border of being normalizable in the sense that it lies at the endpoint of a line of delta-function normalizable operators [30]. It will play a special role in what follows, and we will call this type of operator almost-normalizable. We will flesh out the above analysis considerably in the following sections.

3 Landau-Ginzburg Models

One of our goals in this section is to obtain, in a simple manner, the chiral ring of localized operators in the non-compact Gepner models we described in section 2. For the compact case, this is most carried out by associating a Landau-Ginzburg model to each of the factor conformal field theories. The underlying idea is that at low energies, the Landau-Ginzburg model flows to the conformal field theory that corresponds to the minimal model.

Furthermore, the GSO projection that we discussed for the non-compact Gepner models maps to an orbifold of the Landau-Ginzburg theory. Therefore the techniques derived in [19, 20] to obtain the spectrum in the Landau-Ginzburg models and orbifolds thereof will be crucial for our analysis.

In this section and the next, we give a similar Landau-Ginzburg description of our non-

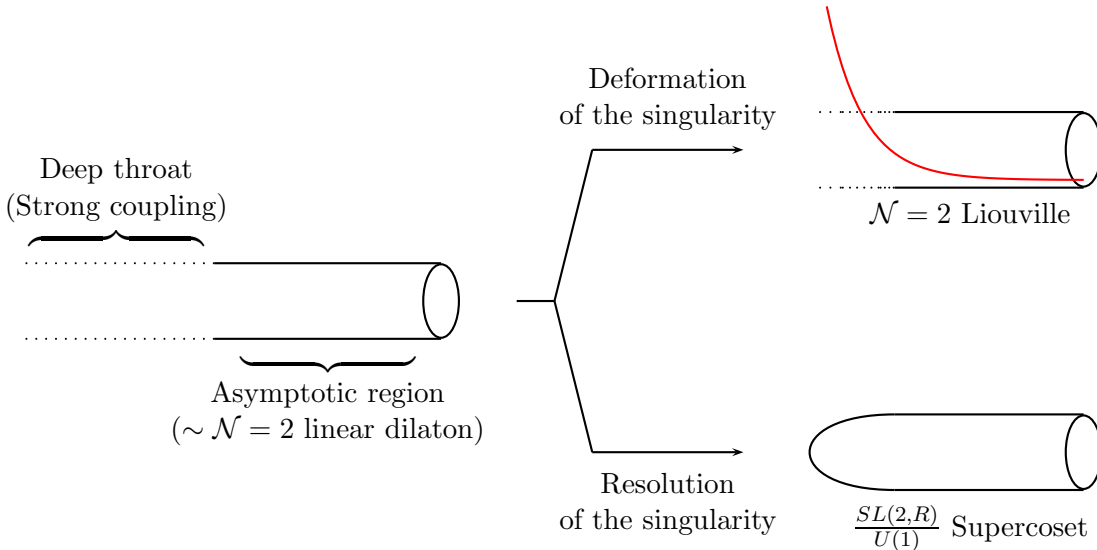


Figure 1: The asymptotic region in a non-compact Gepner model is identical to that of a linear dilaton conformal field theory. The strong coupling singularity can be cured either by turning on a Liouville potential, or by capping the cylinder with a cigar type deformation.

compact Gepner models. We will find that much of the technology used in the compact case can be used for the non-compact case as well. However there are subtle differences in reading off the spectrum, because some of the operators are not normalizable.

3.1 Landau-Ginzburg Potentials For Minimal Models

For $N = 2$ superconformal minimal models, the flow between Landau-Ginzburg and superconformal minimal models is well-studied [33, 34] and we merely give a brief reminder. A Landau-Ginzburg model with $N = (2, 2)$ supersymmetry and a chiral superfield Φ with superpotential

$$W_{MM} = \Phi^k \tag{3.1}$$

flows in the infrared to an $N = 2$ superconformal minimal model. The chiral ring of both models match one-to-one. The chiral unital ring of the Landau-Ginzburg model is $\mathbb{C}[\Phi]/\partial_\Phi W$ which is linearly generated by the $k - 1$ elements $\Phi^0, \Phi^1, \dots, \Phi^{k-2}$, which have (both left- and right-moving) R-charge equal to $0, \frac{1}{k}, \dots, \frac{k-2}{k}$. These match one-to-one to the chiral-chiral primaries of the diagonal minimal model. Further evidence for this identification of the Landau-Ginzburg model fixed point is provided by the matching of the elliptic genus of these models [35].

The T-dual or mirror Landau-Ginzburg model based on an twisted chiral superfield [36] flows to the anti-diagonal minimal model. This can be written as a \mathbb{Z}_k orbifold of the model in equation (3.1). We will discuss such orbifolding methods to compute mirrors in later sections.

We can summarize the chiral ring of the Landau-Ginzburg model by specifying a Poincare polynomial which is the trace over the chiral-chiral ring weighted by the $U(1)$ R-charges [37]:

$$\begin{aligned} Tr_{(c,c)} t^Q \tilde{t}^{\tilde{Q}} &= 1 + (t\tilde{t})^{\frac{1}{k}} + (t\tilde{t})^{\frac{2}{k}} + \dots + (t\tilde{t})^{\frac{k-2}{k}} \\ &= \frac{1 - (t\tilde{t})^{\frac{k-1}{k}}}{1 - (t\tilde{t})^{\frac{1}{k}}}. \end{aligned} \tag{3.2}$$

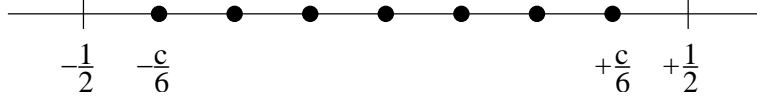


Figure 2: The R-charges of the ground states in the Ramond sector for a $N = 2$ superconformal theory with central charge $c < 3$.

In the Ramond sector, this gives rise to a polynomial that keeps track of the R-charges of the Ramond-Ramond ground states:

$$Tr_{RR} t^{Q\tilde{Q}} = (t\tilde{t})^{-\frac{1}{2}+\frac{1}{k}} + (t\tilde{t})^{-\frac{1}{2}+\frac{2}{k}} + \dots + (t\tilde{t})^{+\frac{1}{2}-\frac{1}{k}}. \quad (3.3)$$

Note that the charges fill out the range from $-c/6$ to $+c/6$, and lie inside the interval $]-\frac{1}{2}, +\frac{1}{2}[$. See figure 2.

3.2 Non-compact Landau-Ginzburg Models

Now we want to discuss the link between the non-compact $N = 2$ superconformal field theories and the IR fixed point of Landau-Ginzburg models with a superpotential of the form:

$$W_{nc} = \Phi^{-l} \quad (3.4)$$

where l is a positive integer. This was introduced⁸ in [25] and we would like to understand how far we can argue for a formal analogy with the compact case, and if possible borrow the techniques that have been extensively used in that context. See also [10, 11] for a more detailed analysis of the renormalization group flow with fixed asymptotics. The central charge of this theory with fixed asymptotics is $c = 3 + \frac{6}{7}$.

It is natural to assume that the field Φ cannot take the value zero, and that moreover the point at infinity should remain a regular point. We can then associate to the model an operator ring $\mathbb{C}[\Phi^{-1}]$ which should again be divided by the ideal generated by the derivative of the superpotential. This gives rise to a ring spanned by the $l + 1$ elements $\Phi^0, \Phi^{-1}, \dots, \Phi^{-l}$. Because the target-space is non-compact, Φ^0 is not normalizable. We exclude the operator from the ring. The ring of elements spanned by $\Phi^{-1}, \Phi^{-2}, \dots, \Phi^{-l}$ is a ring without unit element. This fact contrasts with the compact case, and it is associated to the non-existence of an $SL(2, R)$ invariant ground state in the conformal field theory. The operators $\Phi^{-1}, \Phi^{-2}, \dots, \Phi^{-l}$ have R-charge $\frac{1}{7}, \frac{2}{7}, \dots, \frac{l}{7}$. We can match the operators $\Phi^{-2}, \dots, \Phi^{-l}$ onto the chiral ring of the diagonal linear dilaton theory with $N = 2$ superconformal symmetry (under the assumptions of relevance and normalizability, as discussed in section 2.2). We moreover expect the operator Φ^{-1} to become the almost-normalizable chiral-chiral primary in the infra-red fixed point theory.

Again, we can summarize the chiral-chiral spectrum in a Poincaré polynomial for the (c, c) ring which for the case of (almost-)normalizable elements is:

$$\begin{aligned} Tr_{(c,c)} t^{Q\tilde{Q}} &= (t\tilde{t})^{\frac{1}{7}} + (t\tilde{t})^{\frac{2}{7}} + \dots + (t\tilde{t})^{\frac{l}{7}} \\ &= (t\tilde{t})^{\frac{1}{7}} \frac{1 - (t\tilde{t})}{1 - (t\tilde{t})^{\frac{1}{7}}}. \end{aligned} \quad (3.5)$$

⁸See also e.g. [38, 39] for an older and related use of these models in the context of two-dimensional gravity.

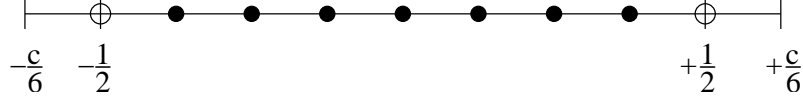


Figure 3: The R-charges of the ground states in the Ramond sector for a $N = 2$ superconformal theory with central charge $c > 3$. There are almost-normalizable ground states at charges $\pm\frac{1}{2}$.

For the strictly normalizable elements, we should use:

$$\begin{aligned} Tr_{(c,c)} t^Q \tilde{t}^{\tilde{Q}} &= (t\tilde{t})^{\frac{2}{l}} + (t\tilde{t})^{\frac{3}{l}} + \dots + (t\tilde{t})^{\frac{l}{l}} \\ &= (t\tilde{t})^{\frac{2}{l}} \frac{1 - (t\tilde{t})^{\frac{l-1}{l}}}{1 - (t\tilde{t})^{\frac{1}{l}}}. \end{aligned} \quad (3.6)$$

Moreover, the normalizable Ramond ground states now have charges that go from $-1/2 + 1/l$ to $+1/2 - 1/l$ which again lie inside the interval $]-\frac{1}{2}, +\frac{1}{2}[$. The almost-normalizable ground state is an outlier at charge $-1/2$. It has a spectrally flowed partner at opposite charge $+1/2$. The Ramond ground states do not reach the charge $-c/6$ and $+c/6$. See figure 3. The R-charges of the strictly normalizable Ramond-Ramond ground states can be coded in the polynomial:

$$Tr_{RR} t^Q \tilde{t}^{\tilde{Q}} = (t\tilde{t})^{-\frac{1}{2} + \frac{1}{l}} + (t\tilde{t})^{-\frac{1}{2} + \frac{2}{l}} + \dots + (t\tilde{t})^{+\frac{1}{2} - \frac{1}{l}}. \quad (3.7)$$

To summarize, we can associate a Landau-Ginzburg model to each factor of a non-compact Gepner model. The total superpotential will be the sum of the individual superpotentials. The Landau-Ginzburg models we discuss will be of the Fermat type. However, we note at this stage that there is a difference between the product of minimal and linear dilaton theories and the corresponding product of Landau-Ginzburg theories. Indeed, while the diagonal A-type minimal models are identified as infra-red fixed points of Landau-Ginzburg models, the non-compact Landau-Ginzburg model gives rise to a deformation of the $N = 2$ linear dilaton theory. To the linear dilaton asymptotics, we add a deforming potential.

So far we have studied simple Landau-Ginzburg theories (and their direct product theories). However, to provide Landau-Ginzburg analogues of the Gepner conformal field theories, we need to discuss orbifolded Landau-Ginzburg models.

4 Landau-Ginzburg Orbifolds

Our discussion of orbifolded Landau-Ginzburg models is mainly based on [19, 20]. The orbifolding can arise due to the GSO projection in string theory, or due to a further geometric orbifolding of the resulting theory. In this section, we start out by discussing the orbifold action as being independent of possible actions on flat space factors, following [20]. We will comment on the relation to the full GSO projection (which also acts on the flat space factors) in the appendix. Since our discussion will be closely related to the long discussion in the literature of the compact case, we will briefly review that discussion and we will only treat in more detail the crucial differences that exist in the non-compact case.

For each compact Landau-Ginzburg model with superpotential $\Phi_i^{k_i}$, there is a canonical diagonal action

$$\Phi_i \rightarrow e^{\frac{2\pi i}{k_i}} \Phi_i, \quad (4.1)$$

which generates a \mathbb{Z}_{k_i} group. The exponent is determined by the $U(1)_R$ charge of the field Φ_i . For every non-compact factor with superpotential $\Phi_j^{-l_j}$, the canonical action is

$$\Phi_j \rightarrow e^{-\frac{2\pi i}{l_j}} \Phi_j. \quad (4.2)$$

We act with the opposite phase, since the $U(1)_R$ charge of the field Φ_j is negative (because of the negative power in the superpotential). We introduce the charges q_i for the fields Φ_i for both compact and non-compact factors, which are equal to

$$\left(\frac{1}{k_1}, \frac{1}{k_2}, \dots; -\frac{1}{l_1}, -\frac{1}{l_2}, \dots \right). \quad (4.3)$$

Then the above actions on the fields can be written as

$$\Phi_i \rightarrow e^{2\pi i q_i} \Phi_i. \quad (4.4)$$

The full symmetry group is then

$$D = \prod_i \mathbb{Z}_{k_i} \times \prod_j \mathbb{Z}_{l_j}. \quad (4.5)$$

Note that it is identical to the group we identified previously in the context of non-compact Gepner models in section 2.1.7.

We study orbifolds of the theory by a subgroup of the above diagonal group D . For instance, we can choose to orbifold by a group generated by a single element, which has different weights in each of the factors, or by a product of such groups. For an element h of the orbifold group, the action on each superfield can be written as

$$\Phi_i \rightarrow e^{2\pi i \Theta_i^h} \Phi_i. \quad (4.6)$$

The phases Θ_i^h parameterize the group elements h .

The integer R-charge orbifold discussed in section 2.1.5 is special, since it is part of the GSO projection. In this case, we orbifold by the group generated by g_0 . The action of this operator on the superfields is coded as $\Theta_i^{g_0} = q_i$.

Our main objective is to compute the number and charges of the chiral/chiral (c, c) and anti-chiral/chiral (a, c) states, as well as their (a, a) and (c, a) partners, in the orbifolded Landau-Ginzburg theory. In particular, those with $U(1)_R$ charges ± 1 will lead to massless fields in spacetime. In the case where the geometric approximation is valid, marginal (c, c) states correspond to complex structure deformations, and marginal (a, c) states to Kähler moduli.

A crucial observation is that for the Calabi-Yau examples we consider in this paper, (c, c) states are in one-to-one correspondence with Ramond-Ramond ground states [37]. More precisely, a Ramond-Ramond ground state becomes a (c, c) state under the action of half-unit left-right symmetric spectral flow. Similarly, (a, c) states are derived from Ramond-Ramond ground states by half-unit left-right antisymmetric spectral flow. It will prove a good strategy to work in the R-R sector rather than in the NS-NS sector. The procedure we will use is the following [20]:

- First identify the unprojected Ramond-Ramond ground states in each twisted sector and compute their R-charge.
- Then flow these states to the NS-NS sector, and keep those that are invariant under the orbifold action.

Let us study the two steps of this procedure in greater detail.

4.1 R-charges of Ramond-Ramond ground states

We first extend a result of reference [19] for the twisted sector Ramond-Ramond ground states. Consider the sector of the theory twisted by h (the following is also valid in the untwisted sector, with $h = 1$). We define a particular Ramond-Ramond ground state $|0\rangle_R^h$, which is the Ramond-Ramond ground state with the lowest left-moving R-charge for the compact factors, and the highest left-moving R-charge for the non-compact factors. The left-moving R-charges with respect to the individual factors of that Ramond-Ramond ground state is:

$$Q = + \sum_{\Theta_i^h \notin Z} \left(\Theta_i^h - [\Theta_i^h] - \frac{1}{2} \right) + \sum_{\Theta_i^h \in Z} \left(q_i - \frac{1}{2} \right), \quad (4.7)$$

and the right-moving R-charge is:

$$\tilde{Q} = - \sum_{\Theta_i^h \notin Z} \left(\Theta_i^h - [\Theta_i^h] - \frac{1}{2} \right) + \sum_{\Theta_i^h \in Z} \left(q_i - \frac{1}{2} \right). \quad (4.8)$$

Here, the expression $[\Theta]$ is defined as the greatest integer smaller than Θ (for Θ not an integer). Remember that Θ_i^h is the phase that defines the action of h on Φ_i , and q_i is the R-charge of Φ_i .

The arguments leading to the first line of these formulae are elaborate [19]. We refer to that reference for details. Note that it is natural to look for the Ramond-Ramond ground state in the h -twisted sector by twisting the left-movers half-way in one direction, and twisting the right-movers half-way in the other direction, due to the symmetry between left- and right-movers in the original theory. The subtraction of the integer part of the twist arises because of the fact that we can otherwise find a state with smaller R-charge, between $-1/2$ and $+1/2$ that will have lower conformal dimension. See also figures 2 and 3. Furthermore, as argued in [19], the R-charges behave very much like fermion number, which is indeed lifted from $-1/2$ in the compact sector, by the contribution of Θ_i^h . The crucial difference with the compact sector is only that for the non-compact sector we need to keep in mind that Θ_i^h is negative, and that therefore it is more natural to think of the state with fermion number or $U(1)_R$ charge moving *down* to a charge just below $+1/2$. That is precisely what is automatically coded in the above formula, since for Θ negative but bigger than -1 , we have that $\Theta - [\Theta] - 1/2 = +1/2 + \Theta$.

The second line in each of these formulae (4.7) and (4.8) arises from spectral flowing the untwisted factor NS-NS ground state to the R-R sector. Note that the superfield living in an untwisted factor can be given a nonzero vev. This is not possible in the twisted factor, since a constant does not satisfy the twisted boundary conditions. In this way, other Ramond-Ramond ground states can be generated in the same sector. For example, if the i -th factor is untwisted, the state $\Phi_i^p |0\rangle_R^h$ (p integer) is another valid Ramond-Ramond ground state. It has left- and right-moving R-charge $(Q + p|q_i|, \tilde{Q} + p|q_i|)$, where we took into account the contribution of Φ_i^p . In a compact factor, p is restricted to the bounds $0 \leq p \leq k_i - 2$. In a non-compact factor, strictly normalizable states have $2 \leq -p \leq l_i$, and almost-normalizable states have $p = -1$. These bounds follow from our discussion in section 3.

The upshot is that the formulas 4.7 and 4.8, derived in [19] for compact models, are also valid for non-compact models.

Once this hurdle is overcome, one can extend the reasoning of [20] to cover the non-compact case as well. We will not repeat the whole analysis here. Let us observe that all the information about the unprojected Ramond-Ramond ground states in the h -twisted sector is conveniently encoded in a Poincaré polynomial equal to:

$$\begin{aligned} \text{Tr}_{R,\text{twisted, unprojected}} t^Q \tilde{t}^{\tilde{Q}} &= \left(\frac{t}{\tilde{t}} \right)^{\sum_{\Theta_i^h \notin Z} (\Theta_i^h - [\Theta_i^h] - 1/2)} (t\tilde{t})^{\sum_{\Theta_i^h \in Z} (q_i - 1/2)} \\ &\times \prod_{\substack{\Theta_i^h \in Z \\ \text{compact} \\ \text{factors}}} \frac{1 - (t\tilde{t})^{\frac{k_i-1}{k_i}}}{1 - (t\tilde{t})^{\frac{1}{k_i}}} \prod_{\substack{\Theta_i^h \in Z \\ \text{noncompact} \\ \text{factors}}} (t\tilde{t})^{\frac{2}{l_i}} \frac{1 - (t\tilde{t})^{\frac{l_i-1}{l_i}}}{1 - (t\tilde{t})^{\frac{1}{l_i}}}. \end{aligned} \quad (4.9)$$

In the untwisted sector, the above analysis simplifies. The particular Ramond-Ramond ground state we discussed earlier had charges $(-c/6, -c/6)$. It is the state one gets by half-unit spectral flow of the NS-NS vacuum. All the superfields are untwisted, and can be given constant values. The relevant Poincaré polynomial is simply the product of the Poincaré polynomials of each factors.

4.2 Spectral flow to the NS-NS sector

In this way we can enumerate all the Ramond-Ramond ground states, and their R-charges. Then we can generate all the NS-NS (anti-)chiral states, by spectral flow.

We obtain (c, c) states by symmetric half-unit spectral flow. Their R-charges are easily computed from those of the Ramond-Ramond ground state: we add $(\frac{c}{6}, \frac{c}{6})$ to the R-charges of the ground state. This operation does not change the twist: h -twisted Ramond-Ramond ground states flow to h -twisted (c, c) states.

In a similar way, we get (a, c) states by anti-symmetric half-unit spectral flow. This time, the Ramond-Ramond ground state R-charges are shifted by $(-\frac{c}{6}, \frac{c}{6})$. Note that anti-symmetric spectral flow changes the twist [19] such that h -twisted Ramond-Ramond ground states flow to hg_0 -twisted (a, c) states.

Among all these states, we keep only those that are invariant under the orbifold action. In the case of the integer R-charge orbifold, the selection is easy: we keep the states that have integer R-charges. But in other cases, the procedure is harder. We refer to [20] for a generic discussion of this projection.

4.3 Normalizability of non-compact twisted states

For the twisted Ramond-Ramond ground states, we encounter a subtle point and this is the crucial difference between the compact and the non-compact case. When we twist a coordinate, and restrict to constant modes, the field is set to zero. This will not give rise to a normalizable state when the Landau-Ginzburg potential has a negative power, since the potential blows up at zero. Although we could therefore immediately discard the states that have a non-compact twisted factor as not being contained in the normalizable spectrum, we advocate keeping an open mind – we will continue the investigation into these non-normalizable states, in view of the possibility that we can tune the coefficient of the negative power potential to zero, which will render these states normalizable.

Strictly speaking, the models where we do take into account such twisted sector deformations should be thought of as existing in the well-defined linear dilaton conformal field theories (which give rise to locally strongly coupled string theory backgrounds). We believe we provide ample justification for this procedure later on. In particular in section 6 we will find that these states are needed in the construction of mirror pairs of conformal field theories, by generalizing the Greene-Plesser prescription of finding mirrors by orbifolding. More precisely, states untwisted in the non-compact directions will be mapped in the mirror model to states twisted in the non-compact directions.

To summarize, the full set of chiral and anti-chiral ring elements of the Landau-Ginzburg orbifold, including those arising in both the untwisted and twisted sectors, is interpreted as the spectrum of the linear dilaton theory. The Landau-Ginzburg model is a complex structure deformation of this linear dilaton background. This deformation removes from the spectrum the RR states twisted in the non-compact directions and the de-singularized string background only contains purely untwisted states. As we will see later on, in the mirror model, the deformation is mapped to a resolution of the theory. The spectrum of the resolved theory will, instead, only contain the states twisted in the non-compact directions.

5 Concrete Models

In this section we will apply what we have learned in the previous sections to some concrete models. We supplement the analysis of the asymptotic partition function of section 2.1 with an analysis of the localized states (which we briefly touched upon in section 2.2). We start out with some observations on the nature of non-compact Gepner models, and how they differ from their compact counterparts. We will then compute the allowed deformations of (c, c) and (a, c) type in particular examples, in the language of orbifolded Landau-Ginzburg models. In the conformal field theory language, the conditions to be satisfied for chiral primaries have been written out in a series of papers [52, 12, 43]. We compare our results with the conformal field theory formalism in appendix A.

5.1 Gepner Points At Large Level

We start out with some comments that allow us to single out some particularly interesting models. Compact Gepner models have factors with a central charge which is always smaller than three. A large level limit for all factors necessarily increases the central charge of the Gepner model, and therefore is not consistent with the criticality condition for string theory. Thus, compact Gepner models are necessarily at large curvature (and small volume).

Non-compact Gepner models are of a different type. In particular we can have non-compact Gepner models that contain factor conformal field theories at central charge smaller *and* larger than three. We can therefore cancel off the difference in a large level limit, if we wish. Assuming that we demand the existence of a limit in which all levels are large, we immediately conclude that such a non-compact Gepner model necessarily has three factors (since the total central charge is $c = 9 = 3 \times 3$).

There are two such classes of models (if we do not admit models with central charge precisely equal to three). One is where we have two minimal model factors and one non-compact factor, and the other has one minimal model factor and two non-compact factors. There are no other possibilities at central charge $c = 9$. (When we consider a non-compact Gepner model at central charge $c = 3.D$, with D an integer different from $D = 3$, there are other possibilities which can also easily be classified.)

The class of models with two minimal models can be parameterized by the integer levels k_1 and k_2 of the minimal models, up to an initial choice of ADE modular invariant and a possible orbifold by a symmetry group. The level l of the non-compact factor is then fixed to be $l = \frac{k_1 k_2}{k_1 + k_2}$ which can be integer or fractional.

The other class of models is parameterized by two levels l_1 and l_2 for the non-compact models, and the combination $k = \frac{l_1 l_2}{l_1 + l_2}$ then needs to be integer, in order for the compact model at level k to exist. The levels l_i can a priori be fractional or real. As we have indicated before, we concentrate on the case where all levels are integer.

Remarks

- We note that a general class of models can be found by demanding $\frac{k_1 k_2}{k_1 + k_2}$ to be integer (with k_1 and k_2 positive integers). Suppose we isolate the greatest common divisor d of $k_1 = d\tilde{k}_1$ and $k_2 = d\tilde{k}_2$ (with \tilde{k}_1 and \tilde{k}_2 mutually prime). Then it can be shown that the level $\frac{k_1 k_2}{k_1 + k_2}$ is integer if and only if d is a divisor of $\tilde{k}_1 + \tilde{k}_2$. That easily generates a large class of models of which we will only study a few.
- We note that although the local curvature would seem to become small in the large level limit, this reasoning does not take into account the GSO orbifold that still needs to be performed. In specific examples it can be checked that the GSO orbifold recreates small radii in the geometry (see e.g. [24][16] for a detailed discussion). We can therefore generically expect the large level limit to correspond to an *orbifolded* weakly curved background.

In the following we will mainly concentrate on the set of models that have the special property of allowing for a large level limit (although our formalism does apply more widely). We study in detail the set of models with three factors and levels $(2k, 2k; k)$ or $(k; 2k, 2k)$ for the minimal model and non-compact factors respectively, and orbifolds thereof. As a warm-up exercise however, we treat the instructive example at complex dimension $D = 2$ with the compact model at level k and the non-compact model at the same level k .

5.2 The $(k; k)$ Model

Let us apply the formalism for orbifolded Landau-Ginzburg models of section 4 to the case of two factors, one compact and one non-compact at equal levels k . We refer to the model as the $(k; k)$ model.

The Landau-Ginzburg model has a potential

$$W_{LG} = \Phi_1^k + \Phi_2^{-k} \quad (5.1)$$

for two chiral superfields Φ_1 and Φ_2 . The orbifold group that is necessary to implement GSO is generated by

$$g_0 : (\Phi_1, \Phi_2) \rightarrow (e^{2\pi i/k} \Phi_1, e^{-2\pi i/k} \Phi_2). \quad (5.2)$$

We will be mostly interested in obtaining the numbers and types of deformations of the conformal field theory. In order to do this, one computes the left and right R-charges of the Ramond-Ramond ground states in all the twisted sectors using equations (4.7) and (4.8). Then, after spectral flow, one can compute the R-charges of the operators in the (c, c) and (a, c) rings. For this $c = 6$ theory, half-unit spectral flow amounts to adding ± 1 unit of R-charge to the RR states.

We recall that for the (a, c) states, asymmetric spectral flow from the RR sector adds a twist by g_0 . We tabulate the R-charges of the relevant states below, and indicate with a star the sectors in which non-zero constant modes can be given to the fields. We label by α the sector twisted by g_0^α .

α	<i>RR</i>	(c, c)	(a, c)
0	$(-1, -1)*$	$(0, 0)*$	$(-1, +1)$
1	$(0, 0)$	$(+1, +1)$	$(-2, 0)*$
$2 \leq \alpha \leq k - 1$	$(0, 0)$	$(+1, +1)$	$(-1, +1)$

(5.3)

We summarize the results:

- In the untwisted sector, the fields can have non-zero constant modes. The Ramond-Ramond ground state flows in the (c, c) ring to the identity operator, with charges $(0, 0)$. We moreover find $k - 1$ marginal (c, c) states in this sector. These arise from the monomials $\Phi_1^n \Phi_2^{-k+n}$ for $n = 0, 1, \dots, k - 2$. They can be checked to be invariant under the orbifold projection.
- Asymmetric spectral flow from the RR untwisted sector gives g_0 -twisted (a, c) states. Therefore we get $k - 1$ marginal (a, c) states in this sector. The fact that these states are marginal is a consequence of the special value of the central charge, $c = 6$.
- For any value of the twist $\alpha = 1, \dots, k - 1$, we have no untwisted fields in the RR sector. Namely the fields Φ_1 and Φ_2 always have twisted boundary conditions in any twisted sector. Using the formula (4.7), we find that the R-charges of the α -twisted sector Ramond ground states is $(\alpha/k - 0 - 1/2) + (-\alpha/k + 1 - 1/2) = 0$ on the left and 0 on the right. We already see a phenomenon typical to our non-compact Gepner models. The twist contribution to the Ramond sector charges can cancel between compact and non-compact factors. We are in a special case, in which the twisted R-charges of all ground states are zero.
- After flowing symmetrically to the NS-NS sector, we find a single (c, c) state with charges $(+1, +1)$ in each twisted sector. They give $k - 1$ marginal (c, c) states in total in the twisted sectors.
- Asymmetric spectral flow of the twisted RR ground states leads to $k - 1$ (a, c) deformations, one in each sector (except for $\alpha = 1$).

Therefore we have a total of $k - 1$ marginal (c, c) and $k - 1$ marginal (a, c) states from the spectral flow of the untwisted RR sector ground states. In the Landau-Ginzburg model with potential $W_{LG} = \Phi_1^k + \Phi_2^{-k}$ these are the only admissible localized modes. The potential term Φ_2^{-k} makes sure that the untwisted polynomials are allowed in the sense that they are normalizable at weak coupling, and have a mild behaviour at the $\Phi_2 \approx 0$ end compared to the potential. These give rise to a $4(k - 1)$ real-dimensional moduli space of backgrounds in string theory with sixteen supercharges. In contrast, the twisted operators are not normalizable in the Liouville deformed model.

5.3 The $(2k, 2k; k)$ Model.

For this slightly more complicated example, we list the full set of (unprojected) (c, c) and (a, c) states and their charges, and then pick out those that are marginal (and invariant

with respect to the orbifold projection). Again, we perform this exercise in the formalism of section 4 for orbifolded Landau-Ginzburg models. We consider a Landau-Ginzburg model with fields $\Phi_{1,2,3}$ and superpotential

$$W_{LG} = \Phi_1^{2k} + \Phi_2^{2k} + \Phi_3^{-k}. \quad (5.4)$$

We perform the integer R-charge orbifold, generated by the g_0 :

$$g_0 : (\Phi_1, \Phi_2, \Phi_3) \rightarrow (e^{2\pi i/2k} \Phi_1, e^{2\pi i/2k} \Phi_2, e^{-2\pi i/k} \Phi_3). \quad (5.5)$$

In order to consider all the marginal operators, we will write down the relevant Poincare polynomials in each sector. First of all, in the untwisted sector we have the (unprojected, strictly normalizable) Poincare polynomial:

$$\left(\frac{1 - (t\tilde{t})^{(2k-1)/2k}}{1 - (t\tilde{t})^{\frac{1}{2k}}} \right)^2 (t\tilde{t})^{\frac{2}{k}} \frac{1 - (t\tilde{t})^{\frac{k-1}{k}}}{1 - (t\tilde{t})^{\frac{1}{k}}} \quad (5.6)$$

which contains (c, c) states only. When we label the twisted sectors by $\alpha = 1, 2, \dots, 2k - 1$, we find that for α smaller than k there are further twisted (c, c) states in the NSNS sector determined by the polynomials:

$$\left(\frac{t}{\tilde{t}} \right)^{-1/2} (t\tilde{t})^{3/2} \quad (5.7)$$

and when α is larger than k by the polynomial

$$\left(\frac{t}{\tilde{t}} \right)^{+1/2} (t\tilde{t})^{3/2}, \quad (5.8)$$

while at $\alpha = k$ we find the polynomial

$$(t\tilde{t})^{-1/k-1/2} (t\tilde{t})^{+3/2} (t\tilde{t})^{\frac{2}{k}} \frac{(1 - (t\tilde{t})^{\frac{k-1}{k}})}{(1 - (t\tilde{t})^{\frac{1}{k}})}. \quad (5.9)$$

where the last factor is due to the fact that Φ_3 is untwisted in this sector. The twisted (a, c) states are determined by the polynomials:

$$\left(\frac{t}{\tilde{t}} \right)^{-2} (t\tilde{t})^0.1 \quad (5.10)$$

when α is smaller than k and

$$\left(\frac{t}{\tilde{t}} \right)^{-1} (t\tilde{t})^0.1 \quad (5.11)$$

when α is larger than k . When $\alpha = k$, we get

$$(t\tilde{t})^{-1/k-1/2} \left(\frac{t}{\tilde{t}} \right)^{-3/2} (t\tilde{t})^{\frac{2}{k}} \frac{(1 - (t\tilde{t})^{\frac{k-1}{k}})}{(1 - (t\tilde{t})^{\frac{1}{k}})}. \quad (5.12)$$

One can straightforwardly determine amongst these the states that are invariant under the orbifold action: they have integer R-charges.

Marginal Deformations

We now want to look for exactly marginal deformations in these rings. These need to have left- and right R-charge equal to ± 1 . As for the $(k; k)$ example, let us tabulate the R-charges of the ground states and their images under spectral flow. Once again, α labels the twist. A star indicates that some fields are untwisted and can be given nonzero vev's.

α	RR	(c, c)	(a, c)
0	$(-3/2, -3/2)*$	$(0, 0)*$	$(-1, 1)$
1	$(-1/2, 1/2)$	$(1, 2)$	$(-3, 0)*$
$2 \leq \alpha < k$	$(-1/2, 1/2)$	$(1, 2)$	$(-2, 2)$
k	$(-1/k - 1/2, -1/k - 1/2)*$	$(-1/k + 1, -1/k + 1)*$	$(-2, 2)$
$k + 1$	$(1/2, -1/2)$	$(2, 1)$	$(-1/k - 2, -1/k + 1)*$
$\alpha > k + 1$	$(1/2, -1/2)$	$(2, 1)$	$(-1, 1)$

(5.13)

The table agrees with the Poincaré polynomials listed previously. We find the following marginal deformations:

- The untwisted (c, c) marginal states are straightforwardly enumerated. They are given by invariant combinations of the Φ_i acting on the vacuum: $\Phi_1^a \Phi_2^b \Phi_3^{-c} |0\rangle_{NS}$, with the bounds $0 \leq a, b \leq 2k - 2$ and $2 \leq c \leq k$. The marginality condition is: $a + b + 2c = 2k$. Let's count these states. For a given c , each a in the range $0 \leq a \leq 2k - 2c$ gives exactly one solution. So the total number of states is:

$$\sharp(c, c) = \sum_{c=2}^k (2k - 2c + 1) = (k - 1)^2 \quad (5.14)$$

- A further search for marginal (c, c) states gives a negative result. When α is smaller than k , we have (c, c) states that survive projection, but they are not marginal since they have charges $(1, 2)$. When $\alpha = k$, the charges left and right can also never be both equal to one. When α is larger than k , the charges are $(2, 1)$ which also never leads to marginality.
- Let us look for marginal (a, c) states in the twisted sector. We get charges $(-2, 2)$ when $\alpha - 1$ is smaller than k , and therefore no marginal states in these sectors. When $\alpha - 1$ is larger than k , we get charges $(-1, +1)$ which are marginal. So we get $(k - 1)$ (a, c) states from the twisted sectors, labeled by $\{k + 2, \dots, 2k\}$. There are no other marginal states in this theory.

In summary, we find $(k - 1)^2$ untwisted marginal (c, c) states, and we find $k - 1$ marginal (a, c) states. Once again, only those states that arise from the spectral flow of RR ground states with untwisted non-compact factors are retained in the theory deformed with the Liouville potential. So all the (c, c) states are in the spectrum of the deformed theory, but none of the (a, c) states are.

5.3.1 Orbifolds

We will now consider orbifolds of the above model. As we will discuss in detail in the next section, this exercise is useful since it generates an infinite number of mirror theories. The logic will be analogous to the Greene-Plesser analysis for the Gepner point in the quintic

Calabi-Yau. Under the hypothesis that the level k is not prime, we can write the level as a product $k = k_1.k_2$ for two positive integers k_1 and k_2 . Then we can perform a \mathbb{Z}_{k_1} orbifold of the three-factor model that we discussed above.

The Landau-Ginzburg model has superpotential

$$W_{LG} = \Phi_1^{2k} + \Phi_2^{2k} + \Phi_3^{-k}.$$

The full symmetry group of W_{LG} is $D = \mathbb{Z}_{2k} \times \mathbb{Z}_{2k} \times \mathbb{Z}_k$, where each factor acts by phase multiplication on one of the superfields. The integer R-charge operator g_0 generates a \mathbb{Z}_{2k} subgroup. It acts as:

$$g_0 : (\Phi_1, \Phi_2, \Phi_3) \rightarrow (e^{\frac{2i\pi}{2k}} \Phi_1, e^{\frac{2i\pi}{2k}} \Phi_2, e^{-\frac{2i\pi}{k}} \Phi_3). \quad (5.15)$$

Now consider the g_1 operator with the following action:

$$g_1 : (\Phi_1, \Phi_2, \Phi_3) \rightarrow (e^{+\frac{2i\pi k_2}{2k}} \Phi_1, e^{-\frac{2i\pi k_2}{2k}} \Phi_2, \Phi_3). \quad (5.16)$$

Earlier we orbifolded the Landau-Ginzburg model by the group generated by g_0 . Consider the group of order $2kk_1$ generated by g_0 and g_1 . We now orbifold the Landau-Ginzburg theory by that group. This is compatible with supersymmetry. Let us find marginal deformations in this orbifold model, following the Landau-Ginzburg method. First we tabulate the R-charges of the Ramond-Ramond ground states. We label the sector twisted by $g_0^\alpha g_1^\beta$ with α and β , within the bounds $0 \leq \alpha \leq 2k - 1$ and $0 \leq \beta \leq k_1 - 1$. A star means that some fields are untwisted.

α	β	RR
$\alpha = 0$	$\beta = 0$	$(-3/2, -3/2)*$
$0 < \alpha < k$	$\beta k_2 < \alpha$	$(-1/2, 1/2)$
$0 < \alpha < k$	$\alpha < \beta k_2$	$(1/2, -1/2)$
$k < \alpha$	$\beta k_2 < 2k - \alpha$	$(1/2, -1/2)$
$k < \alpha$	$2k - \alpha < \beta k_2$	$(-1/2, 1/2)$
$\alpha = 0$	$\beta \neq 0$	$(-1/2 - 1/k, -1/2 - 1/k)*$
$\alpha = k$	β	$(-1/2 - 1/k, -1/2 - 1/k)*$
$\alpha = \beta k_2$	$\beta \neq 0$	$(-1/2 + 1/2k, -1/2 + 1/2k)*$
$\alpha = 2k - \beta k_2$	$\beta \neq 0$	$(-1/2 + 1/2k, -1/2 + 1/2k)*$

Let us count the marginal operators:

- In the untwisted sector, we find (c, c) chiral primaries. Remember that in the model orbifolded by g_0 , the $(k-1)^2$ (c, c) states are labeled by three integers a, b, c , such that $0 \leq a, b \leq 2k-2$, $2 \leq c \leq k$ and $a + b + 2c = 2k$. The g_1 projection keeps only those that have $a \equiv b [2k_1]$.

Let us work at given c . We want to count the number of solutions to the equation $a + b = 2k - 2c$, with $a \equiv b [2k_1]$. We write $b = a + 2dk_1$, with d integer. Then we express a and b in terms of c and d only: $a = k - c - dk_1$, and $b = k - c + dk_1$. The bounds on a and b imply $-k + c \leq dk_1 \leq k - c$. Thus we have one solution for each integer d between $\frac{c-k}{k_1}$ and $\frac{k-c}{k_1}$.

So the total number of (c, c) states is:

$$\sharp(c, c) = \sum_{c=2}^k \left(\left\lfloor \frac{k-c}{k_1} \right\rfloor - \left\lfloor \frac{c-k}{k_1} \right\rfloor + 1 \right) \quad (5.18)$$

where $[x]$ is the largest integer smaller or equal to x , and $\lceil x \rceil$ is the smallest integer bigger or equal to x .

This sum can be evaluated explicitly :

$$\sharp(c, c) = 2 \left((k_2 - 1)(k_1 - 1) + \sum_{\check{c}=2}^{k_2} (k_2 - \check{c})k_1 \right) + k - 1 = k_1 k_2^2 - 2k_2 + 1 \quad (5.19)$$

- In the sector twisted by $g_0^{\alpha \mp 1} g_1^\beta$, we find (c, a) and (a, c) states⁹:
 - If $0 \leq \beta k_2 < \alpha < k$, or $\alpha > 2k - \beta k_2$, we find one marginal (c, a) state. Let's count the number of such twisted sectors. It can be written as:

$$\sharp(c, a) = \sum_{\alpha=1}^{k-1} \left(\left\lfloor \frac{\alpha}{k_2} \right\rfloor + 1 \right) + \sum_{\alpha=k+1}^{2k-1} \left(k_1 - 1 - \left\lfloor \frac{2k - \alpha}{k_2} \right\rfloor \right) \quad (5.20)$$

This sum can be computed explicitly as:

$$\sharp(c, a) = \left((k_2 - 1) \sum_{\hat{\alpha}=1}^{k_1} \hat{\alpha} \right) + \left((k_1 - 1)(k - 1) - (k_2 - 1) \sum_{\check{\alpha}=0}^{k_1-1} \check{\alpha} \right) = k_2 k_1^2 - 2k_1 + 1 \quad (5.21)$$

- Symmetrically, if $0 < \alpha < \beta k_2$, or $k < \alpha < 2k - \beta k_2$, we find one (a, c) state. The same counting shows that there are also $k_2 k_1^2 - 2k_1 + 1$ such sectors.
- Eventually, if $\alpha = 0$, $\alpha = k$ or $\beta k_2 = \pm \alpha [2k]$, we find no marginal deformation.

In summary, we have in this orbifold model:

- $k_1 k_2^2 - 2k_2 + 1$ marginal (c, c) states.
- $k_2 k_1^2 - 2k_1 + 1$ marginal (a, c) states.

Once again, only the (c, c) states are present in the spectrum of the deformed theory.

5.4 The $(k; 2k, 2k)$ Model.

This example will be very similar to the previous one. For this reason our discussion will be brief and we will focus on marginal deformations. The Landau-Ginzburg model has superpotential

$$W_{LG} = \Phi_1^k + \Phi_2^{-2k} + \Phi_3^{-2k} . \quad (5.22)$$

The integer R-charge operator g_0 acts on the superfields as:

$$g_0 : (\Phi_1, \Phi_2, \Phi_3) = (e^{\frac{2i\pi}{k}} \Phi_1, e^{-\frac{2i\pi}{2k}} \Phi_2, e^{-\frac{2i\pi}{2k}} \Phi_3) . \quad (5.23)$$

⁹The $\alpha \mp 1$ occurs due to the shift in the labeling of the twisted sectors when flowing asymmetrically from the RR to the (c, a) or (a, c) sectors.

We tabulate the R-charges of the Ramond ground states and their spectral flows. A star means that some fields are untwisted, and α labels the sector twisted by g_0^α :

α	RR	(c, c)	(a, c)
0	$(-3/2, -3/2)^*$	$(0, 0)^*$	$(-2, 2)$
1	$(1/2, -1/2)$	$(2, 1)$	$(-3, 0)^*$
$2 \leq \alpha < k$	$(1/2, -1/2)$	$(2, 1)$	$(-1, 1)$
k	$(1/k - 1/2, 1/k - 1/2)^*$	$(1/k + 1, 1/k + 1)^*$	$(-1, 1)$
$k + 1$	$(-1/2, 1/2)$	$(1, 2)$	$(1/k - 2, 1/k + 1)^*$
$\alpha > k + 1$	$(-1/2, 1/2)$	$(1, 2)$	$(-2, 2)$

(5.24)

- In the untwisted sector, we find $(k - 1)^2$ (c, c) states.
- In the sector twisted by g_0^α ($0 < \alpha < 2k - 1$), we find one (a, c) state if $2 \leq \alpha \leq k$, and one (c, a) state if $k \leq \alpha \leq 2k - 2$.

To summarize, this model has $(k - 1)^2$ marginal (c, c) deformations and $k - 1$ marginal (a, c) deformations.

5.4.1 Orbifolds

We repeat the analysis of section 5.3.1, and study the orbifolds of this model. The Landau-Ginzburg model has superpotential $W_{LG} = \Phi_1^k + \Phi_2^{-2k} + \Phi_3^{-2k}$. The full group of symmetries of W_{LG} is $\mathbb{Z}_k \times \mathbb{Z}_{2k} \times \mathbb{Z}_{2k}$, where each factor acts by phase multiplication on one superfield.

The integer R-charge operator g_0 generates a \mathbb{Z}_{2k} subgroup and acts as follows:

$$g_0 : (\Phi_1, \Phi_2, \Phi_3) \rightarrow (e^{\frac{2i\pi}{k}} \Phi_1, e^{-\frac{2i\pi}{2k}} \Phi_2, e^{-\frac{2i\pi}{2k}} \Phi_3) \quad (5.25)$$

Now we consider the g_1 operator with the following action:

$$g_1 : (\Phi_1, \Phi_2, \Phi_3) \rightarrow (\Phi_1, e^{-\frac{2i\pi k_2}{2k}} \Phi_2, e^{+\frac{2i\pi k_2}{2k}} \Phi_3) \quad (5.26)$$

As in the $(2k, 2k; k)$ model, we assume that $k = k_1 \cdot k_2$, orbifold the theory by the subgroup generated by g_0 and g_1 and look for marginal deformations. The counting is very similar to the $(2k, 2k; k)$ case. We find

- $k_1 k_2^2 - 2k_2 + 1$ marginal (c, c) states.
- $k_2 k_1^2 - 2k_1 + 1$ marginal (a, c) states.

5.5 The $(3, 3, 3; 2)$ Model

All our previous examples share an interesting feature. The marginal (c, c) operators are obtained by half-unit spectral flow of untwisted RR-ground states. On the other hand, the marginal (a, c) operators are obtained by half-unit asymmetric spectral flow of twisted RR-ground states. A direct consequence is that in these examples, the deformed theory only has (c, c) moduli in its spectrum. This statement looks general, since untwisted ground states have equal left and right R-charges, and tend to flow to chiral operators. Similarly, twisted ground states have different left and right R-charges, and would be expected to flow to anti-chiral operators. However, we will show in the present example that there are exceptions to this rule.

We consider the Gepner model with three compact factors at level 3, and one non-compact factor at level 2. The superpotential of the corresponding Landau-Ginzburg model is

$$W = \Phi_1^3 + \Phi_2^3 + \Phi_3^3 + \Phi_4^{-2} + \Phi_5^2, \quad (5.27)$$

and the model is orbifolded by the group generated by g_0 :

$$g_0 : (\Phi_1, \Phi_2, \Phi_3, \Phi_4, \Phi_5) \rightarrow (e^{\frac{2i\pi}{3}}\Phi_1, e^{\frac{2i\pi}{3}}\Phi_2, e^{-\frac{2i\pi}{3}}\Phi_3, e^{-i\pi}\Phi_4, e^{i\pi}\Phi_5). \quad (5.28)$$

The addition of Φ_5 is the simplest means to ensure that the Calabi-Yau condition is maintained while setting all the phase factors in [20] to zero. Using the by now familiar techniques, we tabulate the R-charges of the ground states in various sectors:

α	RR	(c, c)	(a, c)
0	$(-3/2, -3/2) * \diamond$	$(0, 0) * \diamond$	$(-1, 1)$
1	$(-1/2, 1/2)$	$(1, 2)$	$(-3, 0) * \diamond$
2	$(-1/2, -3/2) *$	$(1, 0) *$	$(-2, 2)$
3	$(-1/2, -1/2) \diamond$	$(1, 1) \diamond$	$(-2, 0) *$
4	$(-3/2, -1/2) *$	$(0, 1) *$	$(-2, 1) \diamond$
5	$(1/2, -1/2)$	$(2, 1)$	$(-3, 1) *$

(5.29)

The star and the diamond respectively mean that the non-compact and the compact fields are untwisted. More precisely, $\Phi_{1,2,3}$ can have zero modes in the $\alpha = 0, 3$ twisted sectors for the (c, c) ring while they can have zero modes in the $\alpha = 1, 4$ twisted sectors in the (a, c) ring. Similarly, $\Phi_{4,5}$ can have zero modes in the $\alpha = 0, 2, 4$ sectors in the (c, c) ring, while it can have zero modes in the $\alpha = 1, 3, 5$ sectors in the (a, c) ring.

From this, we see that there are 2 (c, c) moduli:

$$\Phi_4^{-2}|0\rangle_{c,c}^{\alpha=0} \quad \text{and} \quad |0\rangle_{c,c}^{\alpha=3} \quad (5.30)$$

and 2 (a, c) moduli:

$$|0\rangle_{a,c}^{\alpha=0} \quad \text{and} \quad \Phi_4^{-2}|0\rangle_{a,c}^{\alpha=3}. \quad (5.31)$$

Notice that the (c, c) modulus in the third twisted sector occurs in a sector in which the fields that corresponds to the non-compact direction, Φ_4 , is twisted. Moreover, the (a, c) modulus in the third twisted sector appears while the non-compact direction is untwisted. As a consequence, the theory deformed by the Liouville potential has only one (c, c) modulus in its spectrum, *and* it also has one (a, c) modulus. (On the other hand, the resolved theory will have one (a, c) modulus, together with one (c, c) modulus.) It can be checked by direct calculation that this is consistent with the equations analyzed in [12]. The Gepner model analysis of this model is discussed briefly in appendix A.4.

6 Mirror Symmetry For Non-compact Gepner Models

In this section we address the question of identifying mirror pairs. In the case of compact Gepner models, when we specify the diagonal model as our starting point, we obtain the mirror model by modding out by the maximal discrete subgroup H of the diagonal group G that is consistent with space-time supersymmetry [3]. Subgroups F of H give rise to models that are mirror to models modded out by H/F .

In the following we will argue that non-compact Gepner models behave very similarly, in their undeformed guise. In particular, we shall show that modding out by the maximal subgroup consistent with supersymmetry, we exchange (c, c) and (c, a) deformations of the undeformed theory.

A corollary of this statement is that a theory deformed by a given operator, will map after mirror symmetry to the mirror theory, deformed by the mirror operator. Thus, mirror symmetry applies to the deformed, regular theories as well.

The main difference with the compact models is therefore that the mirror map includes the specification of the action of the mirror map on the deforming operator(s). Naturally, the specification is that one changes the right-moving R-charge of the deforming operator to find the mirror deformation. The mirror map extends to subgroups of H as in the compact case.

We believe it is best to illustrate the above general framework in a few examples. In the following section, we will then revisit these examples and see to what extent we can interpret mirror symmetry of the conformal field theories in a geometric framework.

6.1 Sixteen Supercharges

We recall that compact Gepner models at central charge $c = 6$ lie in the moduli space of $K3$ compactifications of string theory. It is well-known [41] that the mirror transform acts as an automorphism of the $K3$ moduli space and there are special points in the moduli space where there are fixed points. For our non-compact $(k; k)$ model at central charge $c = 6$, we see that in its singular guise, the particular $8(k - 1)$ deformations that we identified are indeed self-mirror. This can be seen in figure 4. Changing the sign of the right-moving R-charge exchanges the two individual sets of $4(k - 1)$ deformation parameters that we distinguished previously. We note that this property of self-mirroring holds only for the singular model.¹⁰

As a consequence, we can discuss mirror symmetry for the weakly coupled deformed model. When we deform the $(k; k)$ model with a Liouville potential (consistent with sixteen supercharges), we are left with $4(k - 1)$ deformation parameters and a regular theory. It is mirror dual to the singular theory deformed by the winding potential (which geometrically gives rise to the cigar theory). The latter theory also has $4(k - 1)$ deformation parameters, which can be mapped individually to their mirror images (using their worldsheet R-charges for each factor of the model).

6.2 Eight Supercharges

For compact Gepner models at central charge $c = 9$, mirror symmetry maps one model onto another, exchanging (c, c) and (c, a) states. We will illustrate that this is the case for non-compact Gepner models as well. First we will treat a case in which we simply mod out by the maximal group, and thus obtain the mirror theory. Then we will show that one can mod out by a subgroup of the maximal subgroup and obtain mirror pairs. We will thus provide large classes of mirror non-compact Gepner models.

¹⁰We do not advocate that the reader take the undeformed (well-defined) conformal field theory as a good description of the strongly coupled string background. We use it as a formal tool in arguing for the precise points of analogy and difference with compact Gepner models.

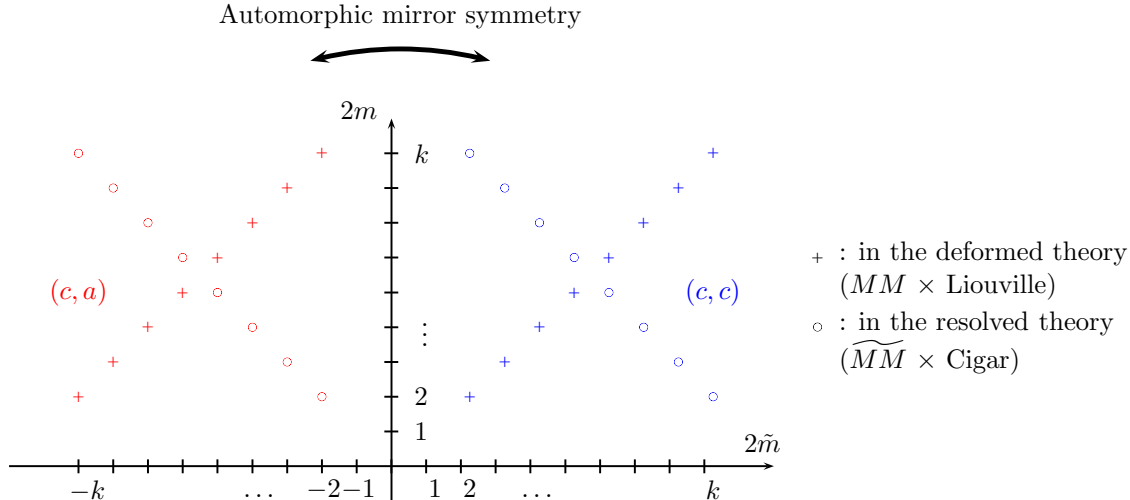


Figure 4: Chiral-chiral and chiral-anti-chiral primaries in the $(k; k)$ model. Each dot corresponds to one chiral primary, identified by its non-compact left- and right-moving quantum numbers $2m$ and $2\tilde{m}$.

6.2.1 The $(k; 2k, 2k)$ Model

We note that the $(k; 2k, 2k)$ model, which is modded out only by the GSO \mathbb{Z}_{2k} group (in the Landau-Ginzburg formulation) has $(k-1)^2$ marginal (c, c) deformations and $k-1$ marginal (a, c) deformations, as discussed in section 5.4. Orbifolds of this model were treated in section 5.4.1. The maximal group that we can divide out by consistent with supersymmetry is the orbifold group when $k_1 = k$ and $k_2 = 1$. Then, substituting in the formulae for the massless moduli computed in that section, we get $k-1$ marginal (c, c) deformations and $(k-1)^2$ marginal (a, c) deformations. The orbifold indeed gives rise to the mirror theory. This is exactly analogous to the Greene-Plesser discussion of mirror conformal field theories associated to compact Calabi-Yau threefolds at a Gepner point.

We want to compare these models to those in the literature. The $(k; 2k, 2k)$ model modded out by the maximal group and deformed by the sum of Liouville potentials corresponds to the non-compact Calabi-Yau studied in [42] to geometrically engineer pure $SU(k)$ gauge theory. The orbifold group restricts all the possible (c, c) deformations to the $k-1$ moduli studied in that paper which span the Coulomb branch of the $SU(k)$ gauge theory. We will discuss the relation between our non-compact Gepner model, the associated Landau-Ginzburg model and this geometry in more detail in the next section.

Moreover, we find that this model is mirror to a model that has no orbifold except the GSO projection, and deformed by the winding condensates in the two non-compact directions. That gives rise to the two-cigar model of [43], as argued in that reference. From our perspective, we see that the double cigar deformations disallow all $(k-1)^2$ marginal (c, c) deformations in the unorbifolded model, and leaves only $k-1$ Kähler deformations. That matches precisely the analysis in [43]. Note that this gives a confirmation of our methodology: the counting in [43] is based on the spectrum identified by considering a regularized partition function [26, 24, 22, 12]. Thus we find that the regularized partition function agrees with our intuitive arguments which find their basis in the Landau-Ginzburg model with negative power potentials (see sections 3 and 4).

As an example of the power of our simple description, we note that the model with

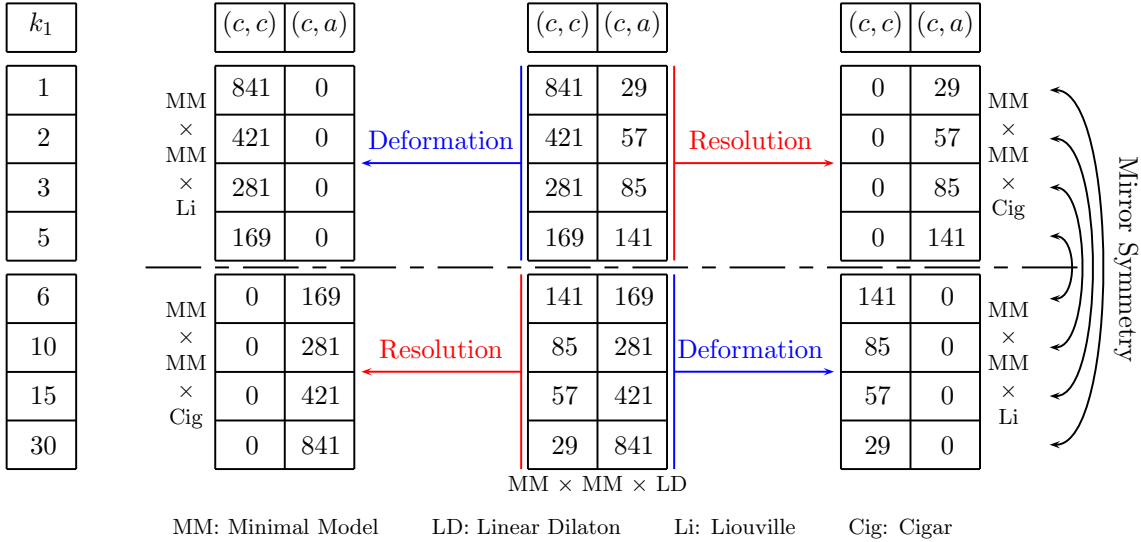


Figure 5: An explicit example: the $(2k, 2k; k)$ models and its orbifolds by \mathbb{Z}_{k_1} , with $k = 30$.

Liouville deformations and no orbifold action is not directly related to the known models described in [42, 43]. Nevertheless, we readily identify its mirror to be the orbifolded theory with cigar deformations in both the non-compact factors.

6.2.2 The Orbifolded $(2k, 2k; k)$ Models

It should be clear now that the examples in sections 5.3.1 and 5.4.1 give rise to two infinite classes of mirror non-compact Gepner models. We will illustrate this for one of the two classes since the other class behaves in almost every respect analogously.¹¹

Recall that the $(2k, 2k; k)$ model allows for a maximal \mathbb{Z}_k orbifold consistent with supersymmetry. When the level k is a product of two positive integers $k = k_1 k_2$, we can orbifold by a non-maximal subgroup $F = \mathbb{Z}_{k_1}$ which gives rise to a model which is mirror to a \mathbb{Z}_{k_2} orbifold of the same model. Indeed, the counting of $(k_1 k_2^2 - 2k_2 + 1)$ marginal (c, c) operators and $(k_2^2 k_1 - 2k_1 + 1)$ marginal (c, a) states in the first model (the \mathbb{Z}_{k_1} orbifold) is precisely the mirror of the counting of the model with \mathbb{Z}_{k_2} orbifold group, as can be seen by exchanging the role of k_1 and k_2 (see figure 5). Thus, we have very simply but explicitly demonstrated the existence of an infinite number of mirror pairs of singular non-compact Gepner models.

We note that the model $(k; 2k, 2k)$ can be treated analogously. The proof of the generic fact that models modded out by a subgroup F of H are mirror to models modded out by H/F runs along very much the same lines as in the compact case [3], for the undeformed theory. For the deformed theory we need to remember that the mirror map will mirror the deformation as well.

7 Mirror Non-compact Geometries and their Relation to \mathbb{C}^n/Γ Orbifolds

In this section we want to discuss some geometric realizations of the mirror map that we identified in the non-compact Gepner models above. We will see that we can identify various

¹¹We will signal the exception in the next section.

models with non-compact Calabi-Yau geometries, and approximate their mirror duals with abelian orbifolds of \mathbb{C}^3 at large levels. At finite level, we find that the results of toric geometry acquire important modifications that lift certain moduli in our models.

7.1 The $(k; k)$ Model

In this model, the space-time background has sixteen supercharges. In analogy with the compact case, we identify the Calabi-Yau manifold that corresponds to the Landau-Ginzburg model by writing down the superpotential (augmented with the appropriate number of quadratic coordinates) in the non-compact weighted projective space $WCIP^4$:

$$w_1^k + w_2^2 + w_3^2 + cw_4^{-k} = 0. \quad (7.1)$$

The constant c (multiplied by the coefficient of the first monomial) measures the strength of the Liouville deformation. By scaling the \mathbb{C}^* valued coordinate w_4 to one, we recuperate the equation:

$$z_1^k + z_2^2 + z_3^2 + c = 0, \quad (7.2)$$

which describes an ALE space which is deformed by c from its singular orbifold limit. We thus associate that geometry to the Landau-Ginzburg model, but we should keep in mind that this association is local, i.e. near the singularity. Asymptotically the spaces differ. We will see an example of the consequences of this difference later on. The matching of the $4(k-1)$ marginal deformations to the geometric moduli is well-known.

7.1.1 The Mirror Theory

The conformal field theory mirror to the above theory was argued to be the $(k; k)$ model with cigar deformation. In the appendix we recall, following [25, 44], that after a single T-duality, this model is mapped to a configuration of NS5-branes spread on a circle in a transverse plane. Moreover, using the explicit geometric description, it can be argued in great detail (see the appendix) that the NS5-branes spread on the circle map under that T-duality to an orbifold singularity of the type $\mathbb{C}^2/\mathbb{Z}_k$ at the tip of the cigar and the center of the minimal model disc. In particular, we see that the \mathbb{Z}_k orbifold that arises from the GSO projection on the side of the cigar mirror conformal field theory acts *geometrically* on the cigar and minimal model coordinates close to the tip of the cigar and the center of the disc.

One should contrast this geometric action to the lack of such an action in the mirror geometry. Moreover, in this example, it becomes manifest that when the cigar/winding deformation is turned on in the singular theory, the deformation caps off the linear dilaton cylinder. As a consequence it gives rise to a (geometric) fixed point which allows for the localization of twisted sector states. That agrees with our prescription for keeping the $4(k-1)$ twisted sector states when turning on the cigar deformation.

Note that there is a one-to-one match of the marginal supersymmetric deformations of the cigar times minimal model conformal field theory to the marginal supersymmetric deformations of the $\mathbb{C}^2/\mathbb{Z}_k$ orbifold (with B -field on the vanishing cycles) [25].

In the strictly infinite level limit, the match is expected, since then the cigar and disc flatten out completely. The two models become identical in that limit. However, at finite level k , the match is due to the rigidity of the sixteen supercharge construction, as will become clear when we discuss models with less supersymmetry.

7.2 The $(k; 2k, 2k)$ Model

Models with eight supercharges will show various new and interesting features. We will discuss two models in detail with increasing level of complexity. The model with levels $(k; 2k, 2k)$ and double Liouville deformation has a singularity that is well-described by a hypersurface in the (non-compact) weighted projective space of the form [43]:

$$w_1^k + w_2^2 + w_3^2 + w_4^{-2k} + w_5^{-2k} = 0, \quad (7.3)$$

where the two coordinates $w_{4,5}$ are \mathbb{C}^* valued. The deforming monomials are in one-to-one correspondence with the $(k-1)^2$ marginal (c, c) deformations that we identified previously. After performing the \mathbb{Z}_k orbifold, we find that only the complex structure deformations of the form $w_1^n (w_4 w_5)^{-k+n}$ for $n = 0, 1, \dots, k-2$ are invariant under the orbifold action. As mentioned earlier, this is precisely the geometry discussed in [42, 11, 43].

7.2.1 The Mirror Theory

Let us now turn to the mirror conformal field theory and see whether we can count the number of Kähler deformations of the mirror theory using geometric means. The first observation we make is that, just as in the case with sixteen supercharges, there is an infinite level limit in which the model flattens out, up to an overall orbifold action. We refer the reader to appendix B for the basic arguments in favour of such a description. In that (strict) limit, the model, locally, near the tips of the cigars and the center of the minimal model disc becomes equivalent to the orbifold $\mathbb{C}^3/\mathbb{Z}_{2k}$. Again, we use that on this side of the mirror symmetry, the GSO projection acts geometrically and infer that the action of the \mathbb{Z}_{2k} on the three factors of \mathbb{C}^3 is weighted as $\frac{1}{2k}(2k-1, 2k-1, 2)$. This orbifold is toric and the number of Kähler deformations of the geometry can be counted using toric geometry techniques¹² as follows.

Consider the supersymmetric orbifold \mathbb{C}^3/Γ , where the orbifold group of order N is generated by

$$\theta : (z_1, z_2, z_3) \longrightarrow (\omega^{a_1} z_1, \omega^{a_2} z_2, \omega^{a_3} z_3) \quad \text{such that} \quad \sum_i a_i = 0 \pmod{N}. \quad (7.4)$$

The counting of Kähler deformations proceeds as follows.

- Consider all powers of θ and list their exponents in multiples of $2\pi i$ such that they fall in the range $1/N \times (0, N-1)$. Label them (g_1, g_2, g_3) .
- The Kähler moduli are in one to one correspondence with those powers of θ that satisfy the following conditions:

$$\sum_{i=1}^n g_i = 1 \quad \text{with} \quad 0 \leq g_i < 1. \quad (7.5)$$

The power of θ tells you in which twisted sector the modulus appears.

Before we proceed further let us also briefly recall how one draws the toric diagram corresponding to the non-compact orbifold. This will turn out to be useful to compare and contrast the spectrum of these non-compact toric orbifolds with the Landau-Ginzburg computation of the spectrum of moduli for the non-compact Gepner models.

¹²See, for instance, [45, 46] and references therein for a review of these methods.

Given an action of $\theta = (\theta_1, \theta_2, \theta_3)$ on \mathbb{C}^3 as above, we first find basis vectors $\{D_1, D_2, D_3\}$ that satisfy

$$\sum_{i=1}^3 \theta_i (D_i)_a = 0 \pmod{N}. \quad (7.6)$$

These three basis vectors generate the toric fan. One solution is $(D_i)_3 = 1 \forall i$. One can find two other linearly independent solutions to this equation. Thus, neglecting the third coordinate of the vectors and plotting only the other two solutions to the above equation, one gets points on a plane. That this must be so follows from the Calabi-Yau condition. These points define the Newton polyhedron corresponding to the non-compact Calabi-Yau. The basis vectors D_i form a cone over the polyhedron which allows one to draw the toric diagram for the Calabi-Yau threefold in the plane. Now, for each power of $\theta^n = (g_1^{(n)}, g_2^{(n)}, g_3^{(n)})$ that satisfies the above two constraints (i.e. for every Kähler deformation), we add another vector (interior or boundary point in the toric diagram) E_n given by

$$E_n = \sum_{i=1}^3 g_i^{(n)} D_i. \quad (7.7)$$

Let us apply the above algorithm to compute the Kähler moduli and draw the toric diagram, for our case where $\Gamma = \mathbb{Z}_{2k}$ (i.e. $N = 2k$) and

$$(\theta_1, \theta_2, \theta_3) = \left(\frac{2k-1}{2k}, \frac{2k-1}{2k}, \frac{2}{2k} \right). \quad (7.8)$$

One can check that there are k Kähler deformations which arise from the twisted sectors $k, k+1, \dots, 2k-1$. This is one more than the number of (c, c) deformations we obtained from the Landau-Ginzburg computation in section 5.4.1. Let us draw the toric diagram corresponding to this orbifold. We choose a basis of vectors

$$D_1 = (0, 1, 1) \quad D_2 = (0, -1, 1) \quad D_3 = (k, 0, 1). \quad (7.9)$$

We add k points, corresponding to the k Kähler deformations, which are elements in the (c, a) ring, in the twisted sectors, whose coordinates are given by

$$E_k = (0, 0, 1), \quad E_{k+1} = (1, 0, 1), \quad E_{k+2} = (2, 0, 1), \quad \dots \quad E_{2k-1} = (k-1, 0, 1). \quad (7.10)$$

These points are plotted in figure 6. Since $E_k = \frac{1}{2}(D_1 + D_2)$ in our \mathbb{Z}_{2k} orbifold it follows that this point will always be on the boundary of the toric diagram.

When we compare the two calculations of the moduli, we see that the difference arises in the $2k-1$ st twisted sector of the GSO orbifold, since, in the conformal field theory, we did not find a marginal Kähler deformation in this twisted sector. Let us study in somewhat more detail how this difference comes about.

It is well known that the points in the toric diagram can also be associated to exceptional divisors of the resolution of the orbifold. This is the twist-field-divisor map discussed in [45]. The topology and intersection numbers of these divisors can be obtained in a straightforward manner by using the dual toric diagram. The boundary point corresponds to non-compact divisors and have the topology $\mathbb{P}^1 \times \mathbb{C}$. Therefore, the existence of the resolution corresponding to E_k in the conformal field theory might seem surprising, given that the (strictly) normalizable deformations in the conformal field theory can be associated to compact cycles in the

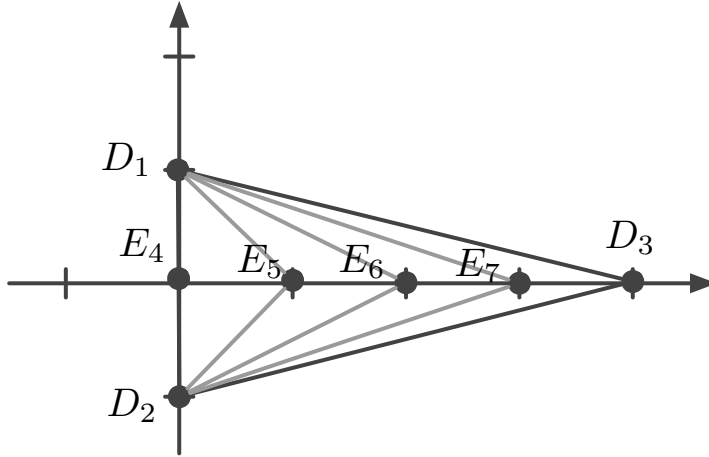


Figure 6: The toric diagram for $\mathbb{C}^3/\mathbb{Z}_{2k}$ for $k = 4$. Note that $E_{k=4}$ corresponds to a boundary point while all other added points lie in the interior of the Newton polyhedron. We have also shown a possible triangulation of the polygon, corresponding to a particular resolution of the singularity.

geometry. This can be understood as follows: the k th power of the orbifold action is trivial on one of the three complex directions in \mathbb{C}^3 , and creates a singularity that stretches along a complex line in \mathbb{C}^3 . The deformation is therefore akin to a Kähler deformation of a \mathbb{C}^2/Γ orbifold, embedded in \mathbb{C}^3 . However, it is important to note that the \mathbb{C} direction that is left invariant in the k th twisted sector, is the direction that is compactified in the conformal field theory by the addition of the Landau-Ginzburg potential. So in the conformal field theory, all the exceptional divisors become compact. A second effect of the compactification is that only $k - 1$ of the deformations are linearly independent. The Landau-Ginzburg counting of chiral primaries gives an easy method to understand which of the exceptional divisors are chosen as a basis in the conformal field theory.

Note that the (c, a) deformation which is the identity operator in the minimal model, sets the volume of the compact factor and simultaneously the volume of the two-cycle at the $\mathbb{C}^2/\mathbb{Z}_2$ singularity. The operator has charges $r = (0, 0, 0; 0; k, k)$ and $\tilde{r} = (0, 0, 0; 0; -k, -k)$ as can be seen from the Landau-Ginzburg model description, or appendix A.3.

7.2.2 The $(2k, 2k; k)$ Model

The toric abelian orbifold that is related to the $(2k, 2k; k)$ model is the same as the one we discussed before. The differences with the previous model lie in the fact that we now compactify two coordinates, which reduces the number of Kähler moduli by two. By analyzing the spectrum of the conformal field theory as before, we find that in the toric diagram corresponding to the flat space orbifold, the twist fields associated to the divisors E_k and E_{k+1} are excluded in the conformal field theory.

However, we gain a Kähler modulus in the 0th twisted sector which sets the overall volume of the two compact factors. It is the identity operator in the minimal model factors, and the winding operator in the cigar factor. It has charges $r = (0, 0, 0; 0; 0, k)$ and $\tilde{r} = (0, 0, 0; 0; 0, -k)$ as can be seen from the Landau-Ginzburg description or from appendix A.2.

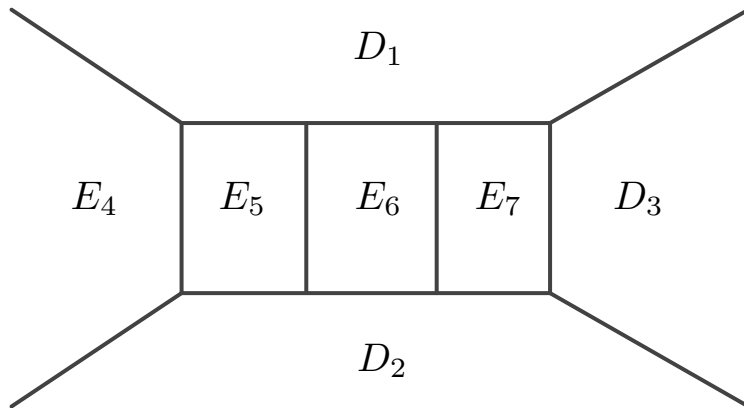


Figure 7: The dual toric diagram for $\mathbb{C}^3/\mathbb{Z}_{2k}$ with $k = 4$. We use the same alphabet to denote the point in the toric diagram and the divisor corresponding to it in the dual toric diagram. Note that E_k (which is E_4 in our case) is non-compact while all the other exceptional divisors are compact.

This is consistent with the picture developed in [13]: the effective string coupling at the tip of the cigar sets the volume of the resolved cycles.

Note that in the previous example, we had a slight refinement of the picture developed in [13]. Namely, in the presence of the two non-compact directions, it is the modulus associated to the \mathbb{Z}_2 orbifold singularity at the tips of the cigars that sets the volume of the internal compact space.

7.2.3 The \mathbb{Z}_{k_1} Orbifold Of The $(k; 2k, 2k)$ Model

In order to understand some more general features of the spectra of the conformal field theory and how they fit into the spectrum of the flat space orbifold approximation, let us study the orbifold models studied in sections 5.3.1 and 5.4.1.

The flat space approximation to the conformal field theory is given by a \mathbb{C}^3/Γ orbifold, generated by the elements

$$\begin{aligned}
 g_0 &= \frac{1}{2k}(2k-1, 2k-1, 2) \quad \text{and} \\
 g_1 &= \frac{1}{2k}(k_2, 2k-k_2, 0).
 \end{aligned}
 \tag{7.11}$$

Using the algorithm discussed earlier, one can easily draw the toric diagram associated to this singularity as in figure 8. The spectrum of the exact conformal field theory has already been discussed in the main part of the paper. If we now plot the spectrum of the exact conformal field theory that corresponds to the $(k; 2k, 2k)$ model along the same lines, we get figure 9. We have shown which elements of the flat space approximation get lifted in going to the exact conformal field theory description.

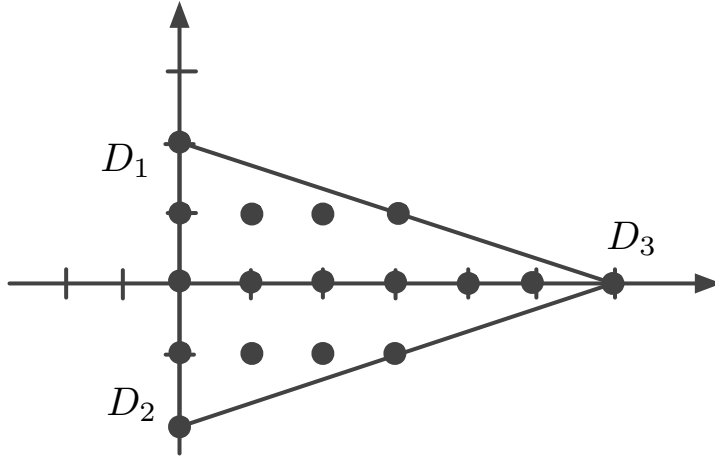


Figure 8: The toric diagram for $\mathbb{C}^3/(\mathbb{Z}_{2k} \times \mathbb{Z}_{k_1})$ with $k = 6$ and $k_1 = 2$.

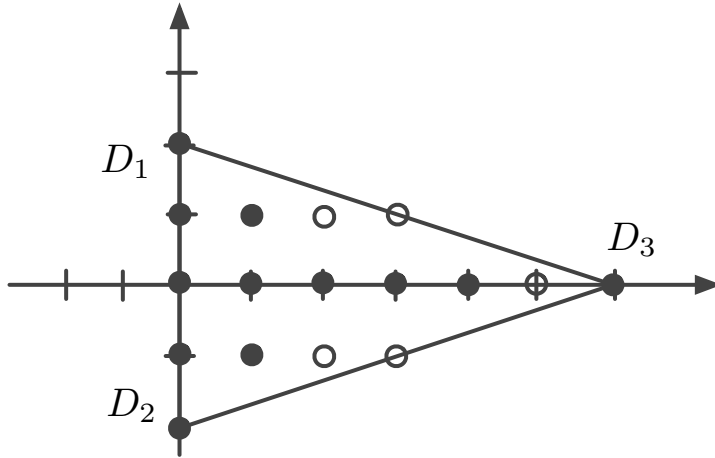


Figure 9: Spectrum of the \mathbb{Z}_{k_1} orbifold of the $(k; 2k, 2k)$ conformal field theory for $k = 6$ and $k_1 = 2$ are denoted by the filled dots. The unfilled dots show those points in the flat space approximation which are not included in the conformal field theory.

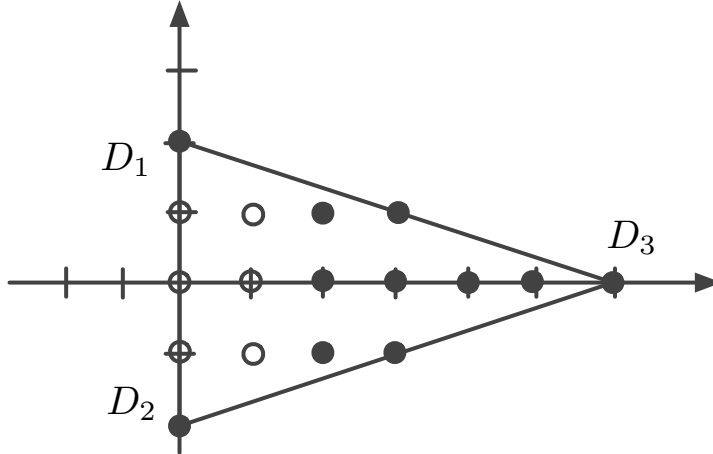


Figure 10: Spectrum of the \mathbb{Z}_{k_1} orbifold of the $(2k, 2k; k)$ conformal field theory for $k = 6$ and $k_1 = 2$ are denoted by the filled dots. The unfilled dots show those points in the flat space approximation which are not included in the conformal field theory.

7.2.4 The \mathbb{Z}_{k_1} Orbifold Of The $(2k, 2k; k)$ Model

For this model the flat space approximation is identical to the one discussed above¹³ and it is drawn in figure 8. The conformal field theory analysis is, however, different and the Kähler deformations which are kept are shown in the figure 10.

We mentioned before that in the toric diagram for the flat space orbifolds, the boundary points correspond to non-compact divisors. Nevertheless as we saw in the simpler orbifold example, in the exact conformal field theory description, some of these directions are compactified. These directions are those along which a potential of the form Φ^n , $n > 0$ is turned on and which flow into a minimal model in the IR. However, the twist fields that correspond to divisors (via the twist-field-divisor map) which extend along directions that remain non-compact should be excluded in the conformal field theory as these do not lead to normalizable deformations. That this is so can be checked in our examples.

For instance, in the $(2k, 2k; k)$ model, in figure 10, the excluded points on the boundary of the toric diagram correspond to Kähler deformations which are in the twisted sectors g_1^β and $g_0^k g_1^\beta$, with $\beta = 1, \dots, k_1 - 1$. Their respective $U(1)$ charges are given by

$$\frac{1}{2k}(\beta k_2, 2k - \beta k_2, 0) \quad \text{and} \quad \frac{1}{2k}(k + \beta k_2, k - \beta k_2, 0) \quad \text{for} \quad n \in \{1, \dots, k_1 - 1\}. \quad (7.12)$$

As one can see, the twist fields are uncharged under the $U(1)$ that acts on the non-compact direction and the divisors that correspond to these fields are non-compact. These are subsequently excluded from the conformal field theory spectrum.

However, further work is required to understand in full generality which states of the flat space orbifold are retained in a given conformal field theory of the type studied in this article.

¹³For the $(2k, 2k; k)$ example, the canonical group element g_0 is given by the inverse of the one we have written here but the group generated and the orbifold of \mathbb{C}^3 associated to it is unchanged.

7.3 Relation to NS5-brane set-ups

The relation of the above orbifold approximations to NS5-brane set-ups has been discussed in the literature. These toric abelian orbifolds of \mathbb{C}^3 can be mapped one-to-one to NS5-brane configurations that wrap holomorphic curves. The holomorphic curves can in turn be described by dimers that are systematically reconstructed from the abelian orbifold group. In the particular case above, one obtains hexagon tilings of the plane with labelings determined by the weights of the GSO projection and further orbifolding. They can be determined by straightforwardly generalizing the examples in [47, 48].

In the sixteen supercharge case, one can show explicitly that the non-compact Gepner model captures the near-horizon doubly scaled limit of the backreacted NS5-brane geometry (as we have recalled in the appendix). In the case of eight supercharges, our non-compact Gepner models capture a near-horizon doubly scaled limit of the backreaction of NS5-branes wrapped on the holomorphic curves coded by the dimer corresponding to our non-compact Gepner model.

8 Conclusions and future directions

We have shown that the Gepner formalism for constructing modular invariant partition functions carries over to the asymptotic partition function of non-compact Gepner models. The analogy was then further developed in a discussion of the symmetry groups of the Gepner models, a classification of subgroups consistent with supersymmetry, and the discussion of how orbifolding by the maximal group can give rise to mirror models.

Secondly, we discussed the deep throat region of the non-compact Gepner models and how to obtain the chiral primary states that are normalizable at weak coupling from the conformal field theory. We then discussed Landau-Ginzburg descriptions of both compact and non-compact Gepner models and extended the existing techniques to analyze Landau-Ginzburg orbifolds such that they applied to the non-compact models under discussion. This led to an intuitive understanding of which modes become normalizable, and which modes are lifted by a momentum or winding potential. The counting of deformations becomes very tractable in the Landau-Ginzburg formalism. For completeness, we matched it onto a more intricate conformal field theory counting.

We used these results to argue that mirror symmetry can be implemented in non-compact Gepner models. When taking into account all possible deformations of the linear dilaton theory, it becomes analogous to the compact case. However, one always needs to keep in mind that the choice of deformation needs to be mirrored when discussing the deformed theories. As expected, we saw that in conformal field theory, mirror symmetry is implemented by a change in sign of the right-moving R-charge. The systematic treatment of symmetry groups allowed us to generate infinite classes of mirror pairs.

Indeed, in non-compact Gepner models, one can cancel off positive and negative contributions to the central charges of the individual factors, thus allowing for infinite classes of models that also have a small curvature limit. In such small curvature limits, we argued that one recuperates flat space with an overall orbifold action. We identified such a limit, along with the orbifold, and showed that the conformal field theory matches with a flat space orbifold in the infinite level limit. At finite level, we identified subtle differences in the spectrum of the conformal field theory and the toric abelian orbifold singularity. It would be interesting to find a general rule that tells us, a priori, which modes of the toric orbifold are retained in the conformal field theory.

There are a large number of future directions that one can pursue. For instance, one can generalize the Landau-Ginzburg models to models with fractional levels in the non-compact directions. One can also apply these conformal field theory techniques to describe the spectrum of chiral primaries and mirror theories for the heterotic string on non-compact Landau-Ginzburg orbifolds.

Another direction that we had in mind while embarking upon this investigation is the following. We have an orbifold approximation to particular non-compact Gepner models. Setting fractional or regular (i.e. physical) branes at such toric orbifold singularities is one way to engineer interesting quiver gauge theories. The toric data allows us to compute the superpotential on the brane at the orbifold singularity using techniques that are very well developed. Extending these results to determine the worldvolume superpotentials for branes in non-compact Gepner models would be extremely interesting as such results are not yet available using the exact boundary state description of D-branes in these models.

Furthermore, Seiberg duality is well-understood in the context of the toric quiver gauge theories [49, 50, 51]. We would like to study whether one can understand Seiberg duality for D-branes in these almost toric spaces [52, 53, 54] microscopically, as in [55, 56]. The fact that we have a microscopic description of the near-horizon doubly scaled limit of these backgrounds as well as a tunable level, should give us further computational control.

Acknowledgments

We are grateful to Agostino Butti, Eleonora Dell’Aquila, Bogdan Florea, Davide Forcella, Amihay Hanany and Ruben Minasian for helpful conversations. Our work was supported in part by the EU under the contract MRTN-CT-2004-005104.

A Non-compact Gepner model analysis

In this appendix we relate the counting of marginal deformations that we performed in a Landau-Ginzburg language to a more elaborate enumeration of states in a standard conformal field theory formalism. See [43] for a detailed discussion and further examples.

A state in the $(k_1, \dots, k_p; l_1, \dots, l_q)$ model (restricted to the internal conformal field theory only) is associated to the left and right charges

$$r = (s_1, \dots, s_{p+q}; n_1, \dots, n_p; 2m_1, \dots, 2m_q)$$

$$\tilde{r} = (\tilde{s}_1, \dots, \tilde{s}_{p+q}; \tilde{n}_1, \dots, \tilde{n}_p; 2\tilde{m}_1, \dots, 2\tilde{m}_q)$$

as well as the compact spins j_1, \dots, j_p and the non-compact spins j_{p+1}, \dots, j_{p+q} . The spins are the same on the left and on the right, since we consider diagonal partition functions. The $2\beta_0$ -orbifold imposes integral R-charges, and allows the difference of left and right charges $r - \tilde{r}$ to be an even multiple of the Gepner vector β_0 . The orbifolds β_i that align the periodicities of the fermions allow additional even differences between the left fermion numbers s_i and the right fermion numbers \tilde{s}_i .

Chiral primary operators are chiral primaries in each conformal field theory factor. From unitarity of the non-compact Gepner models (see appendix C) it follows that in each factor separately we satisfy the equation $\pm Q_i = 2h_i$ for chiral (respectively anti-chiral) primaries and similarly for the right-movers. Marginality of the deformations implies that we need to satisfy the equations

$$Q = 2\beta_0 \cdot r = \pm 1 \quad \tilde{Q} = 2\beta_0 \cdot \tilde{r} = \pm 1.$$

Solving this set of equations is straightforward but tedious because of the equivalences that exist for the minimal model quantum numbers:

$$n_i \equiv n_i + 2k_i, \quad s_i \equiv s_i + 4, \quad (j, n, s) \equiv \left(\frac{k-2}{2} - j, n - k, s + 2\right)$$

The same kind of equivalences hold in the non-compact factor:

$$2m_i \equiv 2m_i + 2l_i, \quad s_i \equiv s_i + 4, \quad (j, 2m, s) \equiv \left(\frac{k+2}{2} - j, 2m - k, s + 2\right)$$

That is one technical reason why the Landau-Ginzburg method is more efficient to count (anti)chiral operators. However it is possible to perform the counting in each individual example that we treated in the bulk of the paper. We do this analysis example by example.

A.1 The $(k; k)$ Model

In the $(k; k)$ model, the Gepner vector is $\beta_0 = (-1, -1; 1; -1)$. Looking for chiral primary operators, we find

- $k - 1$ (c, c) states in the untwisted sector with charges:

$$r = (0, 0; n; k - n) = \tilde{r}, \quad j_1 = n, \quad j_2 = k - n, \quad 0 \leq n \leq k - 2$$

- $k - 1$ (a, c) states in the first twisted sector:

$$r = (0, 0; -n; -k + n), \quad \tilde{r} = r - 2\beta_0, \quad j_1 = n, \quad j_2 = k - n, \quad 0 \leq n \leq k - 2$$

- 1 (c, c) state in each α -twisted sector ($1 \leq \alpha \leq k - 1$):

$$r = (0, 0; \alpha - 1; k - \alpha + 1), \quad \tilde{r} = r - 2\alpha\beta_0, \quad j_1 = \alpha - 1, \quad j_2 = k - \alpha + 1$$

- 1 (a, c) state in each $(\alpha + 1)$ -twisted sector ($1 \leq \alpha \leq k - 1$):

$$r = (0, 0; -\alpha + 1; -k + \alpha - 1), \quad \tilde{r} = r - 2(\alpha + 1)\beta_0, \quad j_1 = \alpha - 1, \quad j_2 = k - \alpha + 1$$

For each (c, c) state we also find a (a, a) state and each (c, a) state is similarly paired with an (a, c) state. It is straightforward to match all these states with the ones we found more fluently in the bulk of the paper with the Landau-Ginzburg methods.

For each state, described by its quantum numbers r , \tilde{r} , j_1 and j_2 , we can write the corresponding closed string vertex operator:

$$V_{r, \tilde{r}}^{j_1, j_2} = V_{n, s_1; \tilde{n}, \tilde{s}_1}^{j_1} V_{2m, s_2; 2\tilde{m}, \tilde{s}_2}^{j_2}. \quad (\text{A.1})$$

Here $V_{n, s_1; \tilde{n}, \tilde{s}_1}^{j_1}$ is a vertex operator of quantum numbers (j_1, n, s_1) in the minimal model, while $V_{2m, s_2; 2\tilde{m}, \tilde{s}_2}^{j_2}$ is a vertex operator of quantum numbers (j_2, n, s_2) in the noncompact factor. If we denote the asymptotic coordinates along the cylinder as ρ and θ and the bosonized complex fermion by H , we have the asymptotic expression for the vertex operators (see e.g. [57]):

$$V_{2m, s; 2\tilde{m}, \tilde{s}}^j = \exp \left[\sqrt{\frac{2}{k}} \left((j-1)\rho + im\theta_L + i\tilde{m}\theta_R \right) + isH_L + i\tilde{s}H_R \right]. \quad (\text{A.2})$$

A.2 The $(2k, 2k; k)$ Model

Let us briefly mention the subtlety that the β_0 vector of Gepner is defined in principle in all factors of the models. The reason we can consider its action separately in the internal factors only without encountering further difficulties lies in the fact that we first of all only consider even multiples of β_0 , and that moreover an even multiple of β_0 is equivalent to the same vector with only non-zero internal entries, up to the vectors β_i . That is true for all three-factor models we consider (and it is therefore also true for the two-factor model when we incorporate two further flat directions).

Having dispensed of that subtlety in comparing the two methods, we can again find the marginal deformations directly in the non-compact Gepner model:

- The $(k-1)^2$ untwisted (c, c) states have quantum numbers:

$$r = (0, 0, 0; a, b, c) = \tilde{r}, \quad j_1 = a, \quad j_2 = b, \quad j_3 = c$$

$$0 \leq a, b \leq 2k - 2, \quad 2 \leq c \leq k, \quad a + b + 2c = 2k$$

- The $k-1$ twisted (a, c) states have quantum numbers:

$$r = (0, 0, 0; -2k + \alpha, -2k + \alpha; k - \alpha), \quad \tilde{r} = r - 2\alpha\beta_0$$

$$j_1 = 2k - \alpha, \quad j_2 = 2k - \alpha, \quad j_3 = \alpha - k, \quad k + 2 \leq \alpha \leq 2k.$$

where α labels the twisted sector in which these states live.

The corresponding closed string vertex operators are given by

$$V_{r, \tilde{r}}^{j_1, j_2, j_3} = V_{n_1, s_1; \tilde{n}_1, \tilde{s}_1}^{j_1} V_{n_2, s_2; \tilde{n}_2, \tilde{s}_2}^{j_2} V_{2m, s_3; 2\tilde{m}, \tilde{s}_3}^{j_3}. \quad (\text{A.3})$$

A.3 The $(k; 2k, 2k)$ Model

The marginal deformations are written as follows:

- The $(k-1)^2$ untwisted (c, c) states have quantum numbers:

$$r = (0, 0, 0; a, b, c) = \tilde{r}, \quad j_1 = a, \quad j_2 = b, \quad j_3 = c$$

$$0 \leq a \leq k - 2, \quad 2 \leq b, c \leq 2k, \quad 2a + b + c = 2k$$

- The $k-1$ twisted (a, c) states have quantum numbers:

$$r = (0, 0, 0; -k + \alpha; -\alpha, -\alpha), \quad \tilde{r} = r - 2\alpha\beta_0$$

$$j_1 = k - \alpha, \quad j_2 = \alpha, \quad j_3 = \alpha, \quad 2 \leq \alpha \leq k$$

where α labels the twisted sectors as before.

The corresponding closed string vertex operators are given by:

$$V_{r, \tilde{r}}^{j_1, j_2, j_3} = V_{n, s_1; \tilde{n}, \tilde{s}_1}^{j_1} V_{2m_1, s_2; 2\tilde{m}_1, \tilde{s}_2}^{j_2} V_{2m_2, s_3; 2\tilde{m}_2, \tilde{s}_3}^{j_3}. \quad (\text{A.4})$$

For the orbifold models as well, one can perform the tedious exercise, thus affirming that the Landau-Ginzburg formalism is indeed more efficient.

A.4 The (3, 3, 3; 2) Model

There is an extra subtlety that we need to address for this model. From the conformal field theory point of view, it is easiest to ignore the quadratic Landau-Ginzburg model with a trivial infra-red fixed point, and to work with an even number of internal conformal field theory factors. It then follows that the vector

$$2\beta_0 = (-2, -2, -2, -2, -2; 2, 2, 2; -2) \quad (\text{A.5})$$

in the full light-cone conformal field theory is not equivalent modulo the vectors β_i to the vector $2\gamma_0 = (0, 0, 0, 0, 0; 2, 2, 2; -2)$ which represents the g_0 action on the Landau-Ginzburg internal conformal field theory. Yet, it can be shown that the Landau-Ginzburg model does correctly count the conformal field theory chiral-chiral and chiral-anti-chiral states. Since it is only the (c, a) state in the 3-twisted sector that is crucial to us in this example, let us show how to identify that state in the conformal field theory. It corresponds to the state with charges $r = (0, 0, 0, 0, 0; 0, 0; 2)$ on the left, as indicated by the Landau-Ginzburg model. The right-moving charges are computed by observing that we are in the 3-twisted sector. We obtain the charge (up to equivalences in the charge lattice) $\tilde{r} = (0, 0, 0, 0, -2; 0, 0; 0)$ (and we remain diagonal in the non-compact quantum number $j = 1$). Indeed, the state with these charges is in the spectrum of the theory.

Note that we had to adjust the precise identification of the state in the conformal field theory. This is typical of the model with an even number of factors. The final vertex operator is chiral and bosonic on the left, and anti-chiral and purely made of fermions on the right.

B T-duality to NS5-branes revisited

In this appendix, we recall the relation of the $(SU(2)/U(1) \times SL(2, R)/U(1))/\mathbf{Z}_k$ coset model to the near-horizon geometry of a particular constellation of NS5-branes [25, 58, 13]. It is useful to revisit this exercise because we will be able to explicitly identify the region of space-time in which the NS5-branes reside with the presence of a patch isomorphic to $\mathbb{C}^2/\mathbf{Z}_k$ in the T-dual. This fact is used as an argument in section 7.

We recall that the supergravity background generated by parallel NS5-branes stretching in the $x^{\mu=0,1,2,3,4,5}$ -directions in the string frame is:

$$\begin{aligned} ds^2 &= \eta_{\mu\nu} dx^\mu dx^\nu + H(x^i) dx^i dx_i \\ e^{2\Phi} &= g_s^2 H(x^i) \\ H_{ijk} &= -\epsilon^l{}_{ijk} \partial_l H(x^i) \end{aligned} \quad (\text{B.1})$$

where the harmonic function H is determined by the positions of the NS5-branes $x_a^{i=6,7,8,9}$:

$$H(x^i) = 1 + \sum_{a=1}^k \frac{\alpha'}{|x^i - x_a^i|^2} \quad (\text{B.2})$$

We concentrate on k NS5-branes spread evenly on a topologically trivial circle of coordinate radius ρ_0 in the (x^6, x^7) plane (see figure 11). We recall from [58, 59] that after the coordinate change $r \geq 0$ and $\theta \in [0, \pi/2]$

$$\begin{aligned} (x^6, x^7) &= \rho_0 \cosh r \sin \theta (\cos \psi, \sin \psi) \\ (x^8, x^9) &= \rho_0 \sinh r \cos \theta (\cos \phi, \sin \phi) \end{aligned} \quad (\text{B.3})$$

and taking a near-horizon doubly scaled limit in which $\rho_0 \rightarrow 0$ and $g_s \rightarrow 0$ and in which $\rho_0 g_s / \sqrt{\alpha'}$ (and α') is kept fixed [13], and after neglecting the localization of the NS5-branes on the circle, we obtain the NS5-brane background:

$$\begin{aligned} ds^2 &= dx^\mu dx_\mu + \alpha' k \left[dr^2 + d\theta^2 + \frac{\tanh^2 r d\phi^2 + \tan^2 \theta d\psi^2}{1 + \tan^2 \theta \tanh^2 r} \right], \\ e^{2\Phi} &= \frac{g_{\text{EFF}}^2}{\cosh^2 r - \sin^2 \theta}, \\ B &= \frac{\alpha' k}{1 + \tan^2 \theta \tanh^2 r} d\phi \wedge d\psi \end{aligned} \quad (\text{B.4})$$

where the effective string coupling constant is

$$g_{\text{EFF}} = \frac{\sqrt{k\alpha'} g_s}{\rho_0}. \quad (\text{B.5})$$

We refer to [59] for the detailed calculation.

A first observation to make is that the NS5-branes are located at $r = 0$ and $\theta = \pi/2$. Moreover, the fact that the coordinate radius of the NS5-brane ring has gone to zero, has been compensated by the fact that the harmonic function and radial metric component has blown up and in such a way that the interior of the NS5-brane ring still has a proper size of order $\sqrt{k\alpha'}$. It is difficult to press together NS5-branes. That's an important aspect of the solution, since in the interior, near $r = 0$ and $\theta = 0$, we simply find a portion of flat space.

After T-duality in the angular direction ψ around which the NS5-branes have been sprinkled, we found the T-dual geometry:

$$\begin{aligned} ds^2 &= \alpha' k \left[dr^2 + \tanh^2 r \left(\frac{d\chi}{k} \right)^2 + d\theta^2 + \cotan^2 \theta \left(\frac{d\chi}{k} - d\phi \right)^2 \right], \\ e^{2\Psi} &= \frac{g_{\text{EFF}}}{k} \frac{1}{\cosh^2 r \sin^2 \theta} \end{aligned} \quad (\text{B.6})$$

where χ is an angle parameterizing the T-dual circle. The background is recognized as a vector \mathbb{Z}_k orbifold of the product of coset conformal field theory geometries $SU(2)_k/U(1) \times SL(2, R)_k/U(1)$.

We want to add a couple of remarks to the analysis in [59] to which we refer the reader for further comments. In particular, we first note the singularity in both the metric and the dilaton at $\theta = 0$. The origin of this singularity is the fact that we have performed an angular T-duality with a fixed point. Around the fixed point, as we have pointed out, the original background behaves like flat space. Thus, the T-dual behavior is recognized as the same type of singularity that one obtains in T-dualizing flat space in cylindrical coordinates. Since the original theory was regular near the origin, we expect the T-dual theory to behave well at this point as well.

On the other hand, we observe that the region at $\theta = \pi/2$ and $r = 0$ where the NS5-branes resides has locally become identical to a $\mathbb{C}^2/\mathbb{Z}_k$ orbifold. Thus, it is the orbifold singularity of order k that codes the presence of the NS5-branes in the T-dual.

We can make the above analysis more precise by performing the following mental exercise. Cut out from the 6 – 7 plane a little disc at the origin. Topologically, the space transverse to the NS5-branes has become $\mathbb{R}^3 \times S^1$, with NS5-branes spread on the S^1 (see figure 11). When we neglect the localization of the NS5-branes on the circle, the configuration is T-dual

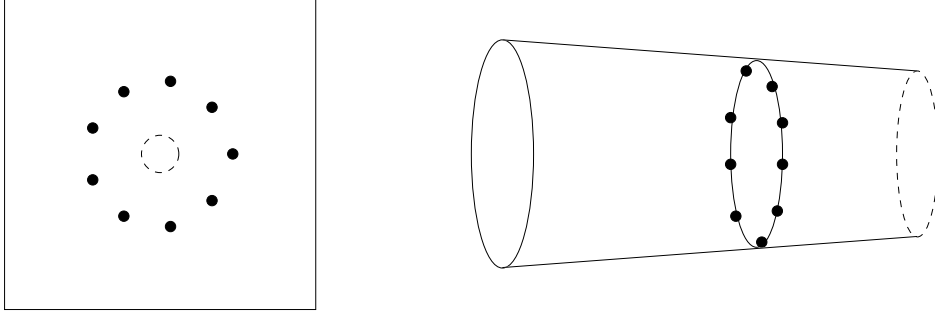


Figure 11: NS5-branes spread on a topologically trivial circle (drawn on the left). When we cut out a little disc at the center, the configuration becomes topologically equivalent to NS5-branes spread on a topologically non-trivial circle (drawn on the right).

to an ALF space [25][44], which in the particular case where the NS5-branes coincide in \mathbb{R}^3 develops a $\mathbb{C}^2/\mathbb{Z}_k$ orbifold singularity. That reasoning is another version of the one above, which uses local fiberwise T-duality. Localizing the NS5-branes in the original geometry on the circle is known to be equivalent to taking into account worldsheet instanton corrections for the ALF space [60][61][62], and this equivalence is conjectured to be valid for the NS5-branes on a topologically trivial circle as well [59].

We take away several facts from this analysis. Firstly, the \mathbb{Z}_k orbifold projection acting on the $SU(2)/U(1) \times SL(2, R)/U(1)$ coset has fixed points and gives rise locally to a physical $\mathbb{C}^2/\mathbb{Z}_k$ singularity that is T-dual to the presence of k NS5-branes. And secondly, in the geometry of the coset conformal field theory, the \mathbb{Z}_k GSO projection acts geometrically on the cigar coordinates, and this in contrast to the fact that the GSO projection in Gepner models does not orbifold the coordinates of weighted projective space. We recalled the above detailed example because we will use these facts as arguments in section 7 and they are particularly manifest in the above example.

C The consequences of unitarity

We list in this appendix a number of properties that hold in unitary modules of the $N = 2$ superconformal algebra, irrespective of the value of the central charge (and in particular also when the central charge is equal or greater than three). Our conventions for the $N = 2$ superconformal algebra coincide with those of [63, 37].

Properties

The following properties hold – the proofs in the references that we give depends only on the unitarity of the representation spaces as we checked on a case-by-case basis:

1. All states in the NS-sector with conformal dimension h and R-charge Q satisfy the inequality $h \geq |Q|/2$ [37].
2. An NS-sector field of conformal dimension h and R-charge Q is a chiral primary if and only if $h = Q/2$ and anti-chiral if and only if $h = -Q/2$ [37].
3. Chiral primary fields satisfy the inequality $h \leq c/6$ [37].

4. Ramond sector ground states have R-charges Q in the range $-c/6 \leq Q \leq +c/6$ [37].
5. An NS-sector state $|\phi\rangle$ satisfies the equations $G_{-l-1/2}^+|\phi\rangle = 0 = G_{l+1/2}^-|\phi\rangle$ if and only if its conformal dimension h and R-charge Q satisfy the relation $h = (l+1/2)Q - c(l^2+l)/6$ [19].
6. A chiral ring exists [37].

Remarks

Note that we performed a non-trivial exercise. For instance, for conformal field theories with central charge $c < 3$, it is argued in [37] that there always exist a chiral primary field in the conformal field theory with conformal dimension $h = c/6$. That is a consequence of the existence of the unit operator in the theory (combined with spectral flow). In other words, there is a normalizable $SL(2, R)$ invariant ground state in these conformal field theories. That is not a consequence of unitarity only, and it does *not* hold generically for unitary $N = 2$ superconformal field theories. In fact, the situation is subtle. For instance there are examples of bulk $N = 2$ superconformal field theories with central charge $c > 3$ for which the unit operator does not exist when the conformal field theory is defined on a Riemann surface without boundary, while it does exist for instance on the boundary of a disc with particular boundary conditions (see e.g. [52][16]). It is due to these kind of subtleties that it is useful to have a (partial) list of properties that we can indiscriminantly use for unitary $N = 2$ theories with any central charge.

References

- [1] S. T. Yau, “Mirror symmetry I,” *Providence, USA: AMS (1998) 444 p*
- [2] B. Greene and S. T. Yau, “Mirror symmetry II,” *Providence, USA: AMS (1997) 844 p. (AMS/IP studies in advanced mathematics. 1)*
- [3] B. R. Greene and M. R. Plesser, *Nucl. Phys. B* **338**, 15 (1990).
- [4] D. Gepner, *Nucl. Phys. B* **296** (1988) 757.
- [5] P. Candelas, X. C. De La Ossa, P. S. Green and L. Parkes, *Nucl. Phys. B* **359** (1991) 21.
- [6] P. Berglund and T. Hubsch, *Nucl. Phys. B* **393**, 377 (1993) [arXiv:hep-th/9201014].
- [7] V. Batyrev, arXiv:alg-geom/9310003.
- [8] T. M. Chiang, A. Klemm, S. T. Yau and E. Zaslow, *Adv. Theor. Math. Phys.* **3**, 495 (1999) [arXiv:hep-th/9903053].
- [9] E. Witten, *Nucl. Phys. B* **403**, 159 (1993) [arXiv:hep-th/9301042].
- [10] K. Hori and C. Vafa, arXiv:hep-th/0002222.
- [11] K. Hori and A. Kapustin, *JHEP* **0211**, 038 (2002) [arXiv:hep-th/0203147].
- [12] T. Eguchi and Y. Sugawara, *JHEP* **0405**, 014 (2004) [arXiv:hep-th/0403193].

- [13] A. Giveon and D. Kutasov, JHEP **9910** (1999) 034 [arXiv:hep-th/9909110].
- [14] K. Hori and A. Kapustin, JHEP **0108**, 045 (2001) [arXiv:hep-th/0104202].
- [15] D. Tong, JHEP **0304**, 031 (2003) [arXiv:hep-th/0303151].
- [16] D. Israel, A. Pakman and J. Troost, Nucl. Phys. B **710**, 529 (2005) [arXiv:hep-th/0405259].
- [17] B. R. Greene, C. Vafa and N. P. Warner, Nucl. Phys. B **324** (1989) 371.
- [18] P. Candelas, M. Lynker and R. Schimmrigk, Nucl. Phys. B **341**, 383 (1990).
- [19] C. Vafa, Mod. Phys. Lett. A **4**, 1169 (1989).
- [20] K. A. Intriligator and C. Vafa, Nucl. Phys. B **339** (1990) 95.
- [21] T. Eguchi and Y. Sugawara, Nucl. Phys. B **577**, 3 (2000) [arXiv:hep-th/0002100].
- [22] A. Hanany, N. Prezas and J. Troost, JHEP **0204**, 014 (2002) [arXiv:hep-th/0202129].
- [23] S. Murthy, JHEP **0311**, 056 (2003) [arXiv:hep-th/0305197].
- [24] D. Israel, C. Kounnas, A. Pakman and J. Troost, JHEP **0406**, 033 (2004) [arXiv:hep-th/0403237].
- [25] H. Ooguri and C. Vafa, Nucl. Phys. B **463**, 55 (1996) [arXiv:hep-th/9511164].
- [26] J. M. Maldacena, H. Ooguri and J. Son, J. Math. Phys. **42**, 2961 (2001) [arXiv:hep-th/0005183].
- [27] D. Gepner and Z. a. Qiu, Nucl. Phys. B **285** (1987) 423.
- [28] B. R. Greene, arXiv:hep-th/9702155.
- [29] J. M. Maldacena, G. W. Moore and N. Seiberg, JHEP **0107** (2001) 046 [arXiv:hep-th/0105038].
- [30] L. J. Dixon, M. E. Peskin and J. D. Lykken, Nucl. Phys. B **325**, 329 (1989).
- [31] S. Gukov, C. Vafa and E. Witten, Nucl. Phys. B **584** (2000) 69 [Erratum-ibid. B **608** (2001) 477] [arXiv:hep-th/9906070].
- [32] A. D. Shapere and C. Vafa, arXiv:hep-th/9910182.
- [33] E. J. Martinec, Phys. Lett. B **217** (1989) 431.
- [34] C. Vafa and N. P. Warner, Phys. Lett. B **218** (1989) 51.
- [35] E. Witten, Int. J. Mod. Phys. A **9**, 4783 (1994) [arXiv:hep-th/9304026].
- [36] M. Rocek and E. P. Verlinde, Nucl. Phys. B **373**, 630 (1992) [arXiv:hep-th/9110053].
- [37] W. Lerche, C. Vafa and N. P. Warner, Nucl. Phys. B **324**, 427 (1989).
- [38] D. Ghoshal and S. Mukhi, Nucl. Phys. B **425** (1994) 173 [arXiv:hep-th/9312189].

- [39] A. Hanany, Y. Oz and M. Ronen Plesser, Nucl. Phys. B **425** (1994) 150 [arXiv:hep-th/9401030].
- [40] D. Ghoshal and C. Vafa, Nucl. Phys. B **453**, 121 (1995) [arXiv:hep-th/9506122].
- [41] P. S. Aspinwall and D. R. Morrison, arXiv:hep-th/9404151.
- [42] W. Lerche, arXiv:hep-th/0006100.
- [43] T. Eguchi and Y. Sugawara, JHEP **0501** (2005) 027 [arXiv:hep-th/0411041].
- [44] D. Kutasov, Phys. Lett. B **383**, 48 (1996) [arXiv:hep-th/9512145].
- [45] P. S. Aspinwall, arXiv:hep-th/9403123.
- [46] D. Lust, S. Reffert, E. Scheidegger and S. Stieberger, arXiv:hep-th/0609014.
- [47] A. Hanany and K. D. Kennaway, arXiv:hep-th/0503149.
- [48] S. Franco, A. Hanany, K. D. Kennaway, D. Vegh and B. Wecht, JHEP **0601** (2006) 096 [arXiv:hep-th/0504110].
- [49] B. Feng, A. Hanany and Y. H. He, Nucl. Phys. B **595** (2001) 165 [arXiv:hep-th/0003085].
- [50] C. E. Beasley and M. R. Plesser, JHEP **0112** (2001) 001 [arXiv:hep-th/0109053].
- [51] F. Cachazo, B. Fiol, K. A. Intriligator, S. Katz and C. Vafa, Nucl. Phys. B **628** (2002) 3 [arXiv:hep-th/0110028].
- [52] T. Eguchi and Y. Sugawara, JHEP **0401**, 025 (2004) [arXiv:hep-th/0311141].
- [53] S. K. Ashok, S. Murthy and J. Troost, Nucl. Phys. B **749**, 172 (2006) [arXiv:hep-th/0504079].
- [54] A. Fotopoulos, V. Niarchos and N. Prezas, JHEP **0510**, 081 (2005) [arXiv:hep-th/0504010].
- [55] S. Murthy and J. Troost, JHEP **0610**, 019 (2006) [arXiv:hep-th/0606203].
- [56] S. K. Ashok, S. Murthy and J. Troost, JHEP **0706**, 047 (2007) [arXiv:hep-th/0703148].
- [57] K. Hosomichi, JHEP **0612** (2006) 061 [arXiv:hep-th/0408172].
- [58] K. Sfetsos, JHEP **9901** (1999) 015 [arXiv:hep-th/9811167].
- [59] D. Israel, A. Pakman and J. Troost, Nucl. Phys. B **722**, 3 (2005) [arXiv:hep-th/0502073].
- [60] R. Gregory, J. A. Harvey and G. W. Moore, Adv. Theor. Math. Phys. **1**, 283 (1997) [arXiv:hep-th/9708086].
- [61] D. Tong, JHEP **0207**, 013 (2002) [arXiv:hep-th/0204186].
- [62] K. Okuyama, JHEP **0508** (2005) 089 [arXiv:hep-th/0508097].
- [63] J. Polchinski, “String theory. Vol. 2: Superstring theory and beyond,” *Cambridge, UK: Univ. Pr. (1998) 531 p*